Simulation-based power analysis and sampling recommendations for IMBCR in Wyoming

Report

June 2026



Bird Conservancy of the Rockies
14500 Lark Bunting Lane
Brighton, CO 80603
303-659-4348
www.birdconservancy.org

Funding agreement: Wyoming PPCAS Code TW SW0 WGBG 100

Table of contents

Table of Contents i

Executive Summary 2

Acknowledgements 4

Introduction 5

Methods 8

Reporting and data repository . . . 8
Simulation framework . . . 8
Focal species . . . 11
Population scenarios . . . 16
Sampling scenarios . . . 18
Baseline sampling . . . 18
Alternative sampling scenarios . . . 18
Simulation approach and estimator properties . . . 20
Statistical power . . . 20
Bias . . . 20

Results 21

Power relationships . . . 21
Sampling effort . . . 21
Sampling distribution . . . 24
Bias . . . 27

Discussion 30

Monitoring recommendations . . . 31
Study limitations and future directions . . . 31

References 32

Appendices 34

Appendix A — Simulation and analysis methods . . . 34

Bird Conservancy of the Rockies

Connecting people, birds and land

Mission: Conserving birds and their habitats through science, education and land stewardship

Vision: Native bird populations are sustained in healthy ecosystems

Bird Conservancy of the Rockies conserves birds and their habitats through an integrated approach of science, education, and land stewardship. Our work radiates from the Rockies to the Great Plains, Mexico and beyond. Our mission is advanced through sound science, achieved through empowering people, realized through stewardship, and sustained through partnerships. Together, we are improving native bird populations, the land, and the lives of people.

Core Values:

1. Science provides the foundation for effective bird conservation.
2. Education is critical to the success of bird conservation.
3. Stewardship of birds and their habitats is a shared responsibility.

Goals:

1. Guide conservation action where it is needed most by conducting scientifically rigorous monitoring and research on birds and their habitats within the context of their full annual cycle.
2. Inspire conservation action in people by developing relationships through community outreach and science-based, experiential education programs.
3. Contribute to bird population viability and help sustain working lands by partnering with landowners and managers to enhance wildlife habitat.
4. Promote conservation and inform land management decisions by disseminating scientific knowledge and developing tools and recommendations.

Suggested Citation:

Latif, Q. S., Z. P. Wallace, L. G. Rossi, J. M. Timmer, and C. E. Latimer. 2026. Simulation-based power analysis and sampling recommendations for IMBCR in Wyoming. Bird Conservancy of the Rockies. Brighton, Colorado, USA.

Contact Information:

Quresh Latif quresh.latif@birdconservancy.org Bird Conservancy of the Rockies 14500 Lark Bunting Lane Brighton, CO 80603 970-482-1707

Executive Summary

Power analyses are a fundamental tool for guiding sampling design for field surveys, but conventional power analyses do not formally account for existing data, necessitating simulation-based power analyses for sampling decisions made in the process of ongoing long-term monitoring. We implemented a simulation-based power analysis to inform sampling allocation decisions made by Wyoming Game and Fish Department (WGFD) for the Integrated Monitoring in Bird Conservation Regions (IMBCR) program in Wyoming.

We simulated IMBCR monitoring for 80 focal species of conservation concern (including 58 state designated Species of Greatest Conservation Need, hereafter SGCN) in Wyoming under seven population trend scenarios (-5% to +5% annual change) and multiple scenarios comprising a range of statewide sampling effort levels and distributions among strata representing different land management agencies and habitats. Simulations spanned the 15-year historical monitoring period (2010–2024), with sampling effort and distribution fixed to match actual levels, and a future 10-year period (2025–2034) over which we simulated various scenarios of sampling effort and distribution. This framework allowed us to evaluate statistical power to discern a range of statewide population trends over the full 25-year period across a realistic set of potential sampling strategies for the future period.

We estimated adequate power (≥ 0.8) to discern statewide trends for 63 of 80 species (43 of 58 SGCN) in Wyoming with any level of sampling considered. Reductions in sampling effort below historical levels compromised statistical power for the most species, particularly when sampling was reduced substantially below historical levels. In contrast, increasing sampling above historical levels yielded comparatively modest gains. The greater cost of decreasing versus benefit with increasing effort suggests historical sampling levels have been close to an inflection point beyond which improvements in statistical power for discerning statewide trends diminish with greater sampling effort (benefits for strata-level trends, reference data for evaluating management, and other monitoring objectives notwithstanding). While our results showed that the baseline effort of 189 grid cells per year (2010–2024) was nearly optimal, they also suggested that recent reductions in effort (125 grid cells in 2025 and 133 in 2026) could significantly compromise our ability to detect trends for priority species if continued.

Within the scenarios considered, statistical power was less sensitive to how sampling was distributed among strata than to total sampling effort. Redistribution of sampling toward strata representing lands managed by specific federal agencies generally resulted in minimal net changes in the number of species with adequate power, though there was some shuffling of which species retained adequate power. Similarly, habitat-focused redistribution scenarios did not strongly improve or compromise overall power, with gains for a few habitat-associated species typically offset by losses for others.

Our results provide actionable guidance for WGFD and other Wyoming funding partners as they make annual decisions about IMBCR funding allocation. Maintaining sampling effort at or near historical levels (about 189 grid cells per year) should be a priority for preserving statistical power for species of conservation concern, and doing so will require commitment from all three

primary funding partners (WGFD, USFS, and BLM). Shifts in sampling distribution among strata managed by different agencies, of the magnitude simulated here, are unlikely to severely compromise statistical power for the number of species with adequate power, provided consistent statewide effort is maintained. Favoring strata representing particular habitat types could further benefit some habitat-associated species (e.g., grassland birds), but increasing effort in favored strata needs to be balanced with maintaining effort in unfavored strata to avoid costs to power for other species. In short, we recommend prioritizing maintenance of existing statewide sampling effort to sustain the value of IMBCR for monitoring species of conservation concern for state and federal agencies. Additionally, allocating more state-funded effort to grassland-dominated strata could achieve power for a grassland bird of high conservation concern (i.e., Lark Bunting). This effort has established a methodology for adaptive power analysis that can be applied to other geographies in the IMBCR program, as well as other long-term monitoring programs for birds and other taxa. All simulation results and code have been archived in data and git repositories, respectively, facilitating further analyses tailored to specific sampling decisions as program conditions evolve.

Acknowledgements

Funding for this work was provided by a grant from the Wyoming Governor's Big Game License Coalition. We thank the participants of the initial workshops in Wyoming and Colorado (Chris Keefe, Melissa Dressen, John Shivik, Sarah Bullock, Ian Abernethy), whose input shaped the monitoring scenarios and species lists that frame these analyses. The Bird Conservancy of the Rockies Biometry team (Bryan Nuse, Qing Zhao, Chris Latimer, and David Pavlacky) provided extensive guidance during the design and implementation of simulations. Matthew McLaren contributed critical input needed for designing monitoring scenarios to appropriately represent the IMBCR program. IMBCR depends on the field technicians who collect the data each season and on the landowners who grant access to their property; this analysis would not have been possible without them. Finally, IMBCR would also not be possible without its many funding and implementation partners. Claude (Anthropic) was used to assist with developing and troubleshooting analysis code, and with drafting and revising portions of this report; the authors reviewed and take full responsibility for all content.

Introduction

Integrated Monitoring in Bird Conservation Regions (IMBCR) is a regional partner-based breeding bird monitoring program administered by Bird Conservancy of the Rockies (hereafter Bird Conservancy) with coverage that includes most of the western U.S.A. from the Great Plains to the Intermountain West. Partners include multiple federal and state agencies and NGOs who contribute funding or field capacity to meet their individual monitoring needs for informing land management within their geographic or programmatic boundaries. By following a common sampling design and survey protocol, partners contribute to broader regional monitoring and benefit from annual analysis and estimation of basic population parameters at multiple scales, including population densities and trends (McLaren et al. 2025, Timmer et al. 2026).

IMBCR grew out of earlier work in Colorado, where Bird Conservancy (then Rocky Mountain Bird Observatory) and its partners developed and implemented the nation's first statewide landbird monitoring program beginning in 1995. Following the North American Bird Conservation Initiative Monitoring Subcommittee's (2007) recommendations for improving avian monitoring, partners redesigned that effort around Bird Conservation Regions (BCRs) as sampling frames stratified by land ownership, and IMBCR began in 2008 with surveys in the Colorado portions of BCRs 16 and 18 and the Wyoming portion of BCR 16 (Pavlacky et al. 2017). Sampling expanded in 2009 to the remaining BCR portions of both states, along with varying portions of other states. Stratification within each state has been revised repeatedly to track partner information needs, particularly during the program's early years (Timmer et al. 2026). Funding for statewide coverage of IMBCR in Wyoming has been shared approximately evenly between the Wyoming Game and Fish Department (WGFD), the U.S. Forest Service (USFS), and the U.S. Bureau of Land Management (BLM), with other partners and granting institutions contributing smaller amounts, and surveys implemented by Bird Conservancy of the Rockies, the Wyoming Natural Diversity Database, and other partners.

IMBCR sampling units are 1-km^2 grid cells, within which surveyors visit evenly spaced survey points arranged in a 4×4 array (Pavlacky et al. 2017). Surveyors record all birds seen or heard at each point in sampled grid cells once per year for 6 minutes during the breeding season (McLaren et al. 2025). Sampling units are selected in a spatially balanced manner (*sensu* Stevens and Olsen (2004)) from within strata, which are mutually exclusive geographic units whose boundaries coincide with areas of distinct management interest (e.g., federal lands, states, and private lands; Figure 1). Strata are nested within larger units of interest, including Bird Conservation Regions at the highest level (hereafter superstrata), allowing derivation of population estimates at various scales of interest (Pavlacky et al. 2017). Partners increasingly seek guidance to identify how many sampling units to survey and how to distribute sampling across strata within regions of interest to cost-effectively meet monitoring objectives.

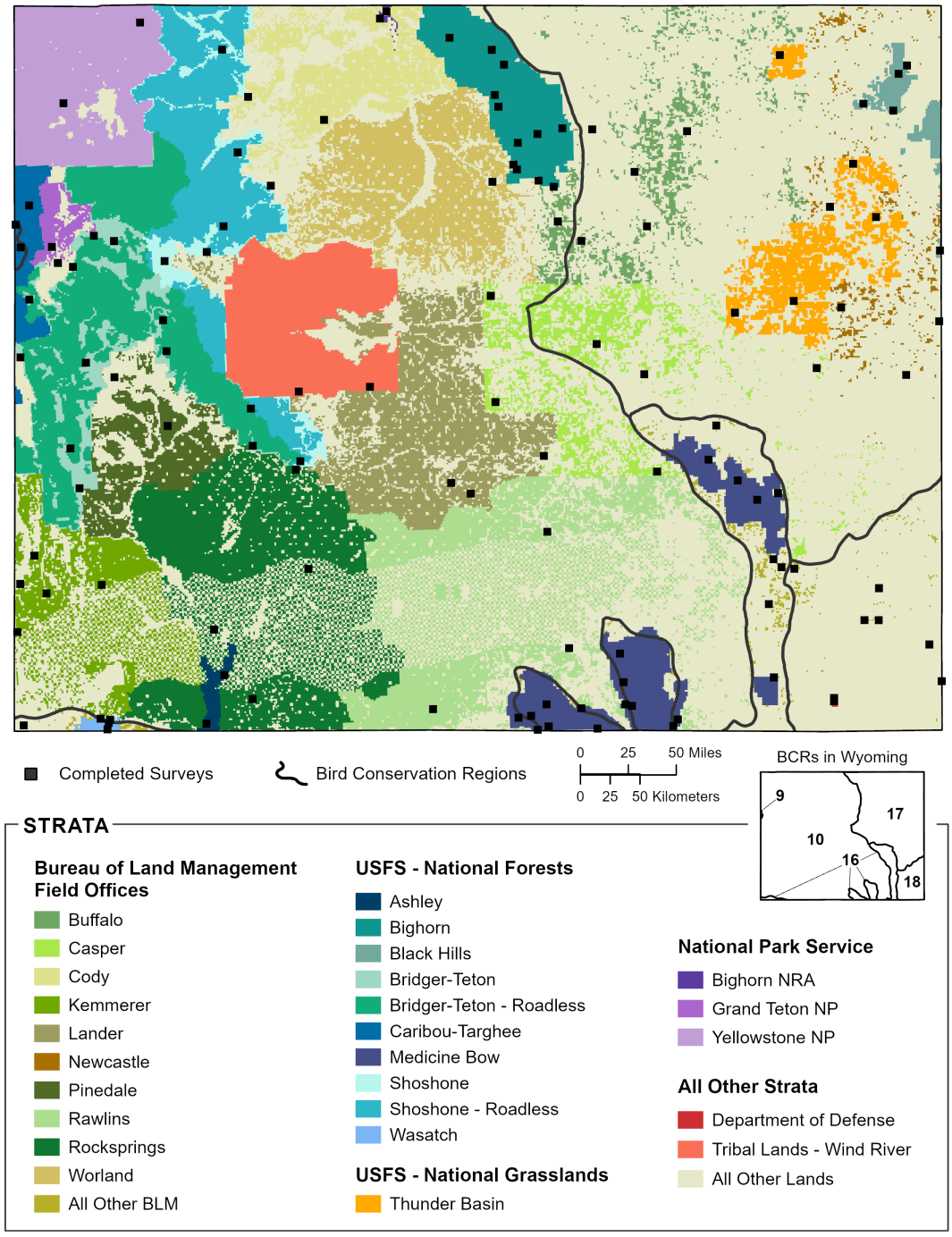


Figure 1. Survey locations and strata for the Integrated Monitoring in Bird Conservation Regions program in Wyoming, 2025. Reproduced from Timmer et al. (2026), Figure 24.1.

Power analyses are a fundamental tool for optimizing sampling and comparing alternative sampling strategies to meet monitoring objectives. The basic approach consists of 1) identifying the effect to be measured (e.g., population trends), 2) specifying the minimum effect size capable of triggering management decisions or changes in management (e.g., 3% annual decline), and 3) calculating the sample size necessary to statistically discern the measured effect (e.g., distinguish the specified trend from a flat trend). Power is the probability that analyzing a dataset of a given size and structure will yield an effect size estimate with sufficient precision to be clearly differentiated from zero, whereby 0.8 is often used as a benchmark for minimum power (Sokal and Rohlf 1995). Analysts seeking to guide sampling design decisions calculate and compare power across scenarios representing alternative options for sampling effort and distribution. Analytical power formulae can produce power relationships capable of generally informing sampling design (e.g., Mackenzie and Royle 2005, Guillera-Arroita and Lahoz-Monfort 2012). However, recent advances in computing allow simulation-based approaches that can customize power analyses to particular monitoring programs (e.g., Andersen and Steidl 2020), potentially providing more realistic and reliable results. In addition to customization, simulations allow comparison of parameter estimates to true values assumed for simulation, enabling us to quantify estimator accuracy along with precision, and thus provide more comprehensive evaluation of sampling design (MacKenzie et al. 2002, Andersen and Steidl 2020).

IMBCR partners increasingly seek information best obtained with customized simulations to inform their particular questions and decisions. Initially, Bird Conservancy biometricians (A. Green and Q. Latif) quantified population density and trend estimator properties for a range of generic hypothetical bird populations aimed at providing generalized sample size guidelines. Latif (2021) built on initial efforts to inform sampling efforts by the Department of Defense at Camp Guernsey, Wyoming, aimed at a particular set of species of interest within a single IMBCR overlay (i.e., a supplemental monitoring effort comparable in scale to a single stratum). These efforts represent important steps towards informing IMBCR sampling decisions for individual background or overlay strata, but partners often have monitoring objectives at the superstratum level and therefore need guidance on sampling effort and distribution across strata within their region of interest. In particular, state wildlife agencies, which are primarily responsible for wildlife population management, need guidance on how to allocate funding across their states in the face of fluctuating and uncertain support from federal funding partners, necessitating more complex simulations than those reported to date. Moreover, sampling decisions need to be made in the context of ongoing monitoring such that simulations should meaningfully represent existing data, necessitating further customization.

We conducted statewide simulations to inform IMBCR sampling and funding allocation decisions made by WGFD. We conducted simulations here in tandem with simulations informing IMBCR sampling in Colorado, the results of which are reported separately (Latif et al. 2026), and we focus on results relevant to WGFD in this report. WGFD relies on IMBCR to monitor population densities and trends for the avian community, with a focus on Species of Greatest Conservation Need (SGCN), and makes yearly decisions about how to allocate available funding for sampling across IMBCR strata within Wyoming while accounting for any fluctuations in funds from federal agencies for sampling on federal public lands. While funding from federal agencies is typically tied to surveys on their lands, WGFD has the flexibility to fund surveys in any stratum, leading to questions about

how best to allocate effort. For this study, we worked with WGFD to identify its most pressing questions when making sampling decisions. Broadly, WGFD was interested in maintaining sampling levels necessary to provide statistical power for discerning population trends at a statewide scale for SGCN, along with species of conservation concern for federal agency partners (hereafter species of interest). The specific questions that we investigated were:

1. How does statistical power to discern statewide population trends for species of interest vary with statewide sampling effort?
    a. In particular, what is the minimum sampling effort needed for adequate power to discern population trends?
    b. Conversely, how much power do we gain by increasing statewide sampling effort beyond historical levels?
2. How does statistical power for statewide trends vary with sampling distribution among strata?
    a. In particular, how would power be affected by allocating a greater proportion of sampling effort to strata representing lands managed by specific agencies as might happen with fluctuations in agency-specific funding?
    b. Conversely, could we gain power by favoring agency-specific strata or strata representing habitats for particular species of interest?

Methods

Reporting and data repository

We supplement reporting broad syntheses of simulation results and implications here with a data repository containing detailed simulation results and metadata (hereafter results repository). In addition to figures and tables illustrating or supporting key methods and findings here, we refer directly to various files or series of files in the results repository by their address. The address of the primary directory for the results repository accompanying this report is `results/`, so files within the results repository may be referenced with `results/[filename]` or `results/[sub-directoryname]/[filename]` for files contained within a sub-directory of the results repository. We refer to multiple versions of a file using brackets containing lists of alternative values within a directory or file path, e.g., `results/.../Figure_power_[80,90,95]CI_stratum.csv` stands for `results/.../Figure_power_80CI_stratum.csv`, `results/.../Figure_power_90CI_stratum.csv`, and `results/.../Figure_power_95CI_stratum.csv`. The `results/Readme.pdf` file provides a detailed catalog and metadata describing the contents of the results repository.

Simulation framework

To meaningfully inform sampling decisions made in the context of ongoing monitoring, we simulated monitoring across periods that spanned the past and future. Simulations proceeded in three phases:

1) we constructed population and sampling scenarios reflecting known species ecology and effort levels of interest to state wildlife agencies, 2) we simulated count data under each scenario using the same hierarchical model applied in the IMBCR annual analysis, and 3) we re-fit that model to simulated data to estimate statistical power and other estimator properties (Appendix A). For the observation period (2010–2024), simulated densities were fixed to posterior median estimates from the annual analysis, and sampling effort (the total number of grid cells) and distribution (relative effort across strata) was fixed to match historical levels in corresponding years. For the future period (2025–2034), we simulated population trajectories under seven annual trend scenarios (-5%, -3%, -1.5%, 0%, 1.5%, 3%, 5%) anchored to the observed trend line (Figure 2), and we varied sampling effort and distribution to represent the range of levels relevant to anticipated sampling decisions (Figure 3). Under this framework, we could examine the implications of sampling decisions regarding future monitoring for statistical power to discern population trends for species of interest across the entire monitoring period (observation + future). Technical details of methods are included in Appendix A and the complete set of species-specific trend figures in the results repository (`results/figures/sim_trends/trend_subplots/`).

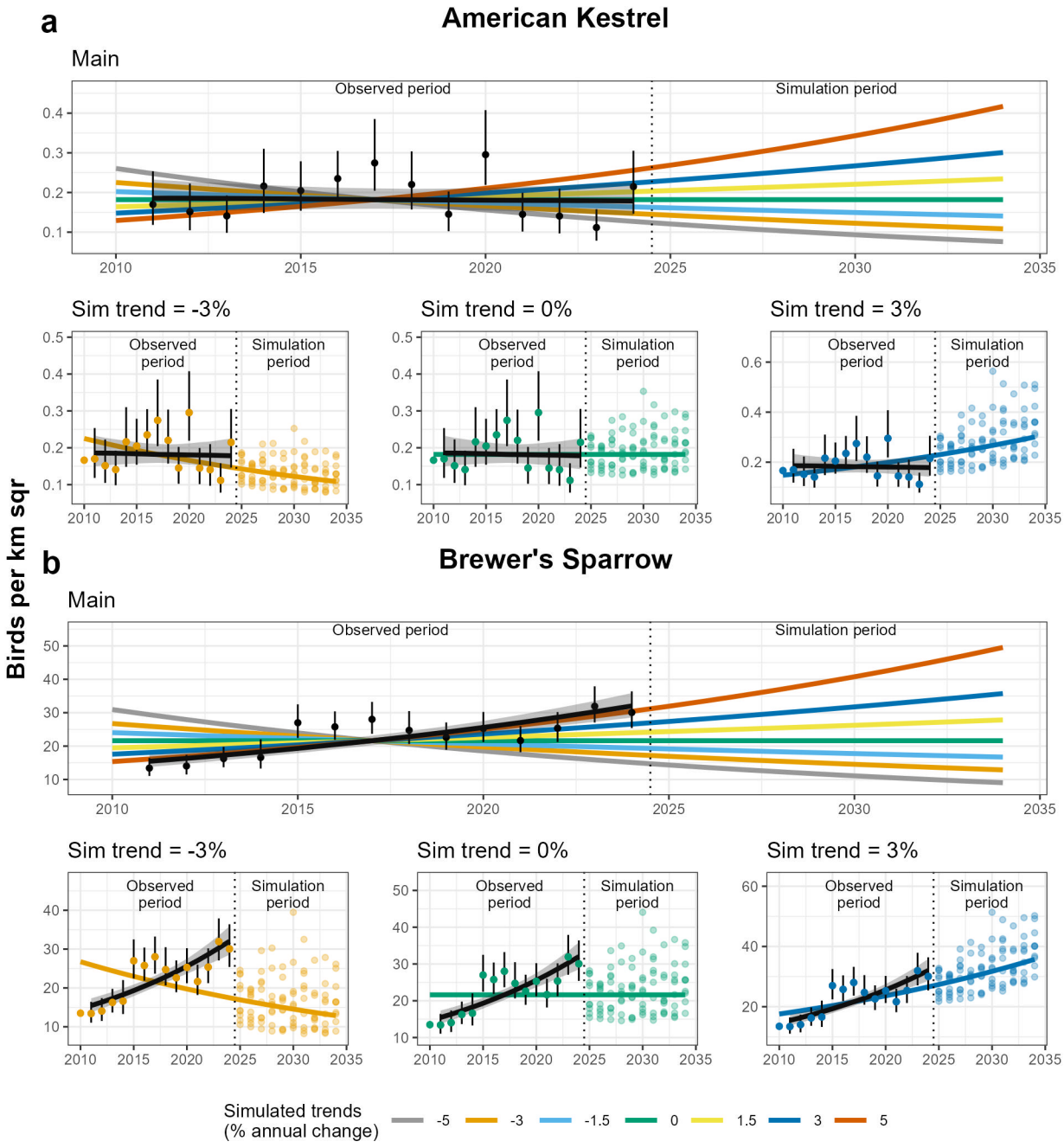


Figure 2. Example illustration of the simulation approach, shown for (a) American Kestrel, a species with a relatively flat historical trend, and (b) Brewer's Sparrow, a species with an increasing historical trend. In each panel, the top plot shows observed density estimates (points) with 95% credible intervals (error bars) and the fitted trend line (black) for the observation period, together with projected trend lines for each of the seven simulated annual trend scenarios (colored lines) applied through the future period; the dotted vertical line marks the boundary between observed and future (simulated) periods. The three smaller plots below each show example simulated densities (points) generated under three representative future-period trend scenarios (-3%, 0%, and 3% annual change).

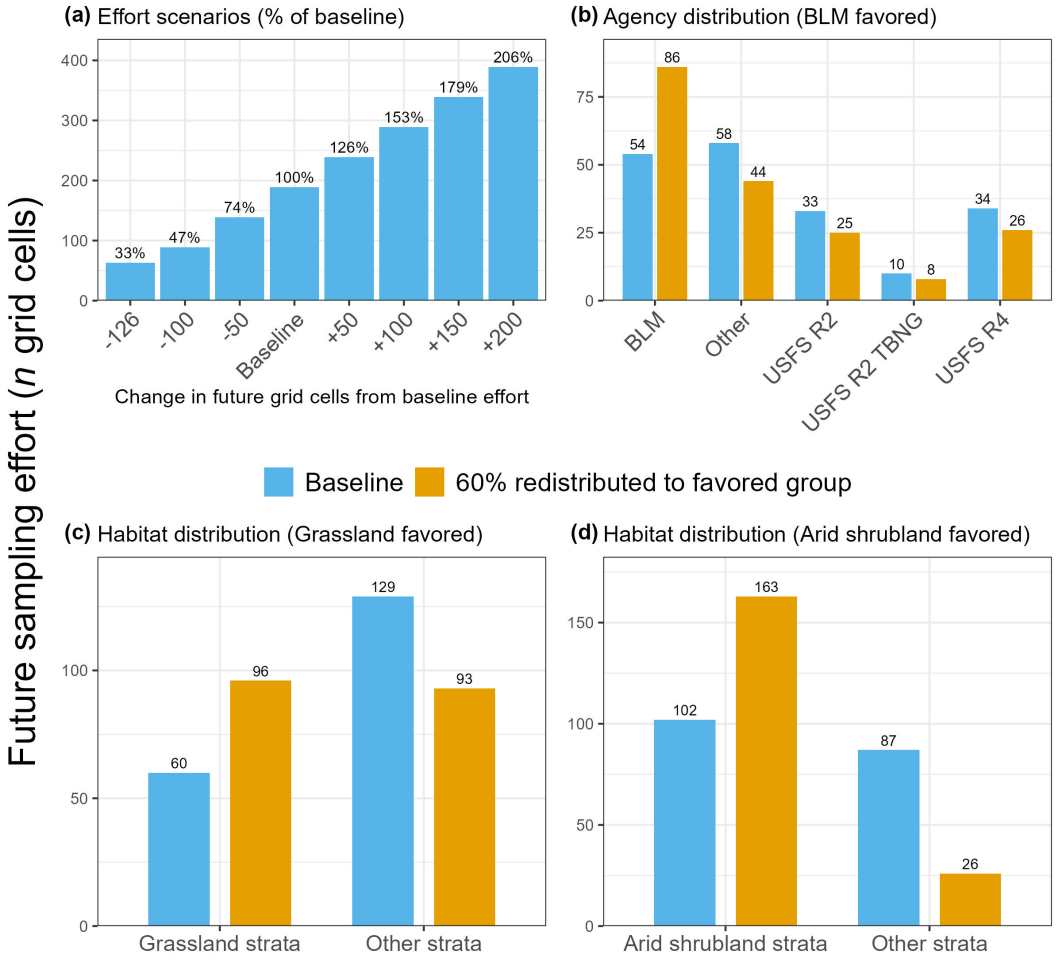


Figure 3. Future scenarios of sampling effort and distribution for power analyses of the IMBCR program in Wyoming. (a) Total statewide grid cells under effort scenarios, expressed as percent of baseline (historical) effort (see Table 2 for baseline effort), ranging from a reduction to a large increase relative to baseline. (b) Agency distribution scenarios, exemplified by redistribution favoring BLM strata by 60%. (c, d) Habitat distribution scenarios, exemplified by redistribution favoring strata representing grasslands (c) and arid shrubland (d; a habitat class primarily dominated by sagebrush). BLM, Grassland, and Arid shrubland scenarios are illustrative examples; analogous scenarios were also simulated for other agencies and habitat types (Table 3 lists all distribution scenarios).

Focal species

We simulated IMBCR monitoring of species of interest as identified by partner agencies and for which IMBCR provides sufficient data to yield abundance and trend estimates (hereafter focal species). We started with species designated as SGCN under the 2017 Wyoming State Wildlife Action Plan (SWAP; Wyoming Game and Fish Department (2017)), proposed as SGCN in the current draft SWAP revision, or included on an informal watch list of common birds in steep decline maintained by WGFD, then added any species not already represented from the lists of Wyoming

BLM Sensitive Species, USFS Regions 2 and 4 Sensitive Species, and Road to Recovery initiative Tipping Point Species. Prior to considering data availability, we identified a list of 101 species (including 78 SGCN) for Wyoming. To analyze abundance for a species, the IMBCR annual analysis requires ≥ 30 detections for that species program wide. Additionally, to be included in Wyoming simulations, we required at least 3 detections recorded within Wyoming samples. After applying these criteria, we retained 80 focal species (including 58 SGCN) for Wyoming simulations (Table 1; `results/reference/Species_list_analysis.csv`). We note that this list represents a relatively small subset of species in Wyoming for which IMBCR provides statewide density estimates (224 species in 2025, of which 126 estimates were informative with CV $\leq 50\%$) and statewide trend estimates (230 species in 2025). For a full list of covered species, visit the RMADC (Rocky Mountain Avian Data Center 2.0 2024).

Table 1. Candidate focal species considered for Wyoming simulations (101 candidates (78 SGCN), of which 80 (58 SGCN) were retained for simulation; Included = yes). Species were excluded (Included = no) if they did not meet the minimum IMBCR detection thresholds required for analysis (≥ 30 detections program-wide and ≥ 3 detections within Wyoming "Sum of counts"; see Focal species). "Status" indicates the primary reason each species was identified as a candidate (see footnote for codes; "–" for candidates not assigned a status). Each species has one status; SGCN species were identified first, so species in the other categories are not SGCN and were added to the list over and above the SGCN species. "Associated habitats" lists the habitat classes with which each species was associated for defining habitat-oriented sampling distribution scenarios (described in Alternative sampling scenarios). "Sufficient power" indicates whether a species ever achieved accurate power ≥ 0.8 to discern a simulated statewide trend in at least one scenario, across all trend scenarios, sampling scenarios, and credible intervals (80, 90, and 95%) considered ("–" for excluded candidates, which were not analyzed).

Common name	Taxonomic name	Code	Status	Sum of counts	Associated habitats	Included	Sufficient power
American Barn Owl	*Tyto alba*	BANO	Prop. SGCN	–	–	no	–
American Bittern	*Botaurus lentiginosus*	AMBI	SGCN	–	–	no	–
American Goshawk	*Accipiter atricapillus*	AGOS	SGCN	59	Conifer forest	yes	yes*
American Kestrel	*Falco sparverius*	AMKE	SGCN	827	Rangeland	yes	yes
American Pipit	*Anthus rubescens*	AMPI	SGCN	782	Alpine	yes	yes
American Three-toed Woodpecker	*Picoides dorsalis*	ATTW	WGFD	257	Conifer forest	yes	yes
American White Pelican	*Pelecanus erythrorhynchos*	AWPE	SGCN	197	Riparian marsh water	yes	no
Ash-throated Flycatcher	*Myiarchus cinerascens*	ATFL	SGCN	198		yes	no
Baird's Sparrow	*Centronyx bairdii*	BAIS	SGCN	28	Rangeland, Grassland	yes	yes*
Bald Eagle	*Haliaeetus leucocephalus*	BAEA	WGFD	71		yes	yes*

(continued)

Common name	Taxonomic name	Code	Status	Sum of counts	Associated habitats	Included	Sufficient power
Bewick's Wren	*Thryomanes bewickii*	BEWR	SGCN	1,600	Conifer forest, Pine juniper	yes	yes
Black-backed Woodpecker	*Picoides arcticus*	BBWO	SGCN	29		yes	yes*
Black-billed Cuckoo	*Coccyzus erythropthalmus*	BBCU	SGCN	–	–	no	–
Black-chinned Hummingbird	*Archilochus alexandri*	BCHU	SGCN	4		yes	no
Black-crowned Night Heron	*Nycticorax nycticorax*	BCNH	SGCN	–	–	no	–
Black-throated Gray Warbler	*Setophaga nigrescens*	BTYW	SGCN	445	Conifer forest, Pine juniper	yes	yes
Black Rosy-Finch	*Leucosticte atrata*	BLRF	SGCN	161	Alpine	yes	yes*
Black Tern	*Chlidonias niger*	BLTE	SGCN	3		yes	no
Blue-gray Gnatcatcher	*Polioptila caerulea*	BGGN	SGCN	865	Conifer forest, Pine juniper, Dry conifer forest	yes	yes
Blue Grosbeak	*Passerina caerulea*	BLGR	SGCN	50		yes	yes*
Bobolink	*Dolichonyx oryzivorus*	BOBO	SGCN	–	–	no	–
Boreal Owl	*Aegolius funereus*	BOOW	SGCN	–	–	no	–
Brewer's Sparrow	*Spizella breweri*	BRSP	SGCN	45,207	Rangeland, Arid shrubland	yes	yes
Brown-capped Rosy-Finch	*Leucosticte australis*	BCRF	SGCN	–	–	no	–
Burrowing Owl	*Athene cunicularia*	BUOW	SGCN	81	Rangeland, Grassland	yes	yes*
Bushtit	*Psaltriparus minimus*	BUSH	SGCN	–	–	no	–
Calliope Hummingbird	*Selasphorus calliope*	CAHU	SGCN	27		yes	no
Canyon Wren	*Catherpes mexicanus*	CANW	SGCN	94	Conifer forest, Dry conifer forest	yes	yes
Caspian Tern	*Hydroprogne caspia*	CATE	SGCN	–	–	no	–
Cassin's Sparrow	*Peucaea cassinii*	CASP	USFS	281	Rangeland, Grassland	yes	no
Chestnut-collared Longspur	*Calcarius ornatus*	CCLO	SGCN	472	Rangeland, Grassland	yes	yes
Chimney Swift	*Chaetura pelagica*	CHSW	R2R	3		yes	no
Chipping Sparrow	*Spizella passerina*	CHSP	WGFD	8,311	Conifer forest	yes	yes
Clark's Grebe	*Aechmophorus clarkii*	CLGR	SGCN	–	–	no	–
Clark's Nutcracker	*Nucifraga columbiana*	CLNU	SGCN	5,486	Conifer forest	yes	yes
Common Loon	*Gavia immer*	COLO	SGCN	–	–	no	–
Common Nighthawk	*Chordeiles minor*	CONI	SGCN	2,243	Rangeland, Arid shrubland	yes	yes

(continued)

Common name	Taxonomic name	Code	Status	Sum of counts	Associated habitats	Included	Sufficient power
Common Yellowthroat	*Geothlypis trichas*	COYE	SGCN	384	Riparian marsh water	yes	yes
Dark-eyed Junco	*Junco hyemalis*	DEJU	WGFD	17,860	Conifer forest	yes	yes
Dickcissel	*Spiza americana*	DICK	SGCN	4		yes	no
Evening Grosbeak	*Coccothraustes vespertinus*	EVGR	Prop. SGCN	304	Conifer forest	yes	yes
Ferruginous Hawk	*Buteo regalis*	FEHA	SGCN	86	Rangeland, Grassland, Arid shrubland	yes	yes
Field Sparrow	*Spizella pusilla*	FISP	Prop. SGCN	184	Rangeland, Grassland	yes	yes
Flammulated Owl	*Psiloscops flammeolus*	FLOW	SGCN	–	–	no	–
Forster's Tern	*Sterna forsteri*	FOTE	SGCN	5		yes	no
Franklin's Gull	*Leucophaeus pipixcan*	FRGU	SGCN	10		yes	no
Golden-crowned Kinglet	*Regulus satrapa*	GCKI	WGFD	198	Conifer forest	yes	yes
Golden Eagle	*Aquila chrysaetos*	GOEA	SGCN	162	Rangeland, Arid shrubland	yes	yes
Grasshopper Sparrow	*Ammodramus savannarum*	GRSP	SGCN	4,908	Rangeland, Grassland	yes	yes
Gray Vireo	*Vireo vicinior*	GRVI	SGCN	–	–	no	–
Great Blue Heron	*Ardea herodias*	GBHE	SGCN	118		yes	yes
Great Gray Owl	*Strix nebulosa*	GGOW	SGCN	–	–	no	–
Greater Sage-Grouse	*Centrocercus urophasianus*	GRSG	SGCN	291	Rangeland, Arid shrubland	yes	yes
Hermit Thrush	*Catharus guttatus*	HETH	WGFD	7,903	Conifer forest	yes	yes
Juniper Titmouse	*Baeolophus ridgwayi*	JUTI	SGCN	118		yes	no
Lark Bunting	*Calamospiza melanocorys*	LARB	Prop. SGCN	24,185	Rangeland, Grassland	yes	yes
Lewis's Woodpecker	*Melanerpes lewis*	LEWO	SGCN	21		yes	yes*
Loggerhead Shrike	*Lanius ludovicianus*	LOSH	SGCN	682	Rangeland, Arid shrubland	yes	yes
Long-billed Curlew	*Numenius americanus*	LBCU	SGCN	173	Rangeland, Grassland, Arid shrubland	yes	yes
MacGillivray's Warbler	*Geothlypis tolmiei*	MGWA	SGCN	2,331	Conifer forest, Hardwood forest, Riparian marsh water	yes	yes
Merlin	*Falco columbarius*	MERL	SGCN	15		yes	no
Mountain Bluebird	*Sialia currucoides*	MOBL	WGFD	4,745	Pine juniper, Arid shrubland	yes	yes
Mountain Plover	*Anarhynchus montanus*	MOPL	SGCN	243	Rangeland, Grassland, Arid shrubland	yes	yes*

(continued)

Common name	Taxonomic name	Code	Status	Sum of counts	Associated habitats	Included	Sufficient power
Northern Harrier	*Circus hudsonius*	NOHA	USFS	321	Rangeland, Grassland	yes	yes
Northern Pintail	*Anas acuta*	NOPI	Prop. SGCN	164	Riparian marsh water	yes	yes*
Northern Pygmy-Owl	*Glaucidium gnoma*	NOPO	SGCN	9		yes	yes*
Olive-sided Flycatcher	*Contopus cooperi*	OSFL	USFS	1,003	Conifer forest	yes	yes
Peregrine Falcon	*Falco peregrinus*	PEFA	SGCN	35	Conifer forest	yes	yes*
Pinyon Jay	*Gymnorhinus cyanocephalus*	PIJA	Prop. SGCN	648	Conifer forest, Pine juniper, Arid shrubland	yes	yes
Purple Martin	*Progne subis*	PUMA	SGCN	–	–	no	–
Pygmy Nuthatch	*Sitta pygmaea*	PYNU	SGCN	68	Conifer forest, Dry conifer forest	yes	yes*
Red-eyed Vireo	*Vireo olivaceus*	REVI	SGCN	80	Conifer forest, Dry conifer forest	yes	yes*
Red-headed Woodpecker	*Melanerpes erythrocephalus*	RHWO	SGCN	370	Grassland	yes	yes
Red Crossbill	*Loxia curvirostra*	RECR	SGCN	6,273	Conifer forest	yes	yes
Rufous Hummingbird	*Selasphorus rufus*	RUHU	SGCN	34		yes	no
Sage Thrasher	*Oreoscoptes montanus*	SATH	SGCN	16,389	Rangeland, Arid shrubland	yes	yes
Sagebrush Sparrow	*Artemisiospiza nevadensis*	SABS	SGCN	10,768	Rangeland, Arid shrubland	yes	yes
Savannah Sparrow	*Passerculus sandwichensis*	SAVS	WGFD	2,215	Riparian marsh water	yes	yes
Scott's Oriole	*Icterus parisorum*	SCOR	SGCN	–	–	no	–
Sharp-tailed Grouse	*Tympanuchus phasianellus*	STGR	SGCN	138	Rangeland, Grassland	yes	yes*
Short-eared Owl	*Asio flammeus*	SEOW	SGCN	78	Rangeland, Arid shrubland	yes	yes*
Snowy Egret	*Egretta thula*	SNEG	SGCN	–	–	no	–
Snowy Plover	*Charadrius nivosus*	SNPL	SGCN	–	–	no	–
Steller's Jay	*Cyanocitta stelleri*	STJA	WGFD	279	Conifer forest	yes	yes
Swainson's Hawk	*Buteo swainsoni*	SWHA	SGCN	184	Rangeland, Grassland	yes	yes
Thick-billed Longspur	*Rhynchophanes mccownii*	TBLO	SGCN	1,467	Rangeland, Arid shrubland	yes	yes
Trumpeter Swan	*Cygnus buccinator*	TRUS	SGCN	6		yes	no
Upland Sandpiper	*Bartramia longicauda*	UPSA	SGCN	750	Rangeland, Grassland	yes	yes
Virginia's Warbler	*Leiothlypis virginiae*	VIWA	SGCN	36	Conifer forest	yes	yes
Virginia Rail	*Rallus limicola*	VIRA	SGCN	–	–	no	–

(continued)

Common name	Taxonomic name	Code	Status	Sum of counts	Associated habitats	Included	Sufficient power
Western Cattle-Egret	*Bubulcus ibis*	CAEG	SGCN	–	–	no	–
Western Grebe	*Aechmophorus occidentalis*	WEGR	SGCN	55	Riparian marsh water	yes	no
Western Kingbird	*Tyrannus verticalis*	WEKI	WGFD	1,635	Rangeland, Grassland	yes	yes
White-faced Ibis	*Plegadis chihi*	WFIB	SGCN	60		yes	no
White-winged Crossbill	*Loxia leucoptera*	WWCR	Prop. SGCN	43	Conifer forest	yes	yes*
Williamson's Sapsucker	*Sphyrapicus thyroideus*	WISA	SGCN	121	Conifer forest, Hardwood forest	yes	yes
Willow Flycatcher	*Empidonax traillii*	WIFL	SGCN	136	Riparian marsh water	yes	yes
Wilson's Phalarope	*Phalaropus tricolor*	WIPH	Prop. SGCN	364	Riparian marsh water	yes	yes
Wilson's Warbler	*Cardellina pusilla*	WIWA	WGFD	597	Conifer forest, Riparian marsh water	yes	yes
Woodhouse's Scrub-Jay	*Aphelocoma woodhouseii*	WOSJ	SGCN	31		yes	no
Yellow-billed Cuckoo	*Coccyzus americanus*	YBCU	SGCN	–	–	no	–

Status codes:
SGCN = designated as a Species of Greatest Conservation Need by the Wyoming Game and Fish Department (WGFD) under the 2017 Wyoming State Wildlife Action Plan (WGFD 2017); Prop. SGCN = proposed as SGCN in the current draft State Wildlife Action Plan revision; WGFD = included on an informal WGFD watch list of common birds in steep decline; USFS = USFS Region 2 or 4 Sensitive Species; R2R = Road to Recovery initiative Tipping Point Species (a dash indicates excluded candidates, which were not assigned a status).
* Met the sufficient-power threshold only with bias correction applied; not met without correction (see the Bias section under Results).

Population scenarios

Simulated populations for focal species were defined by annual statewide population densities, strata-level population densities, and spatial variability within strata (i.e., variability among grid cells). We assumed statewide population densities arose from three fundamental processes: 1) average population size, 2) a population trend, and 3) environmental stochasticity or annual variation around the average size and trend. Considering our interest in measuring statistical power to discern trend, trend (process 2) represented the fundamental effect size for evaluating power and as such, distinguished alternative population scenarios for any given species. We calibrated remaining parameters to match sampled populations as represented in available IMBCR data.

We simulated populations under seven possible trend scenarios: -5%, -3%, -1.5%, 0%, +1.5%, +3%, and +5% annual change (hereafter simulated trends). The range of simulated trends qualitatively matched the range of species-specific statewide (posterior median) trends estimated from the IMBCR

annual analysis during the observation period for Wyoming. We constructed simulated populations based on species density (birds per km^2) and trend estimates from the IMBCR annual analysis. Having defined baseline sampling to exclude monitoring prior to 2010, however (described under Sampling scenarios, Baseline sampling), we implemented a modified version of the annual analysis that excluded data collected prior to the observation period. The model and procedure for analyzing observation-period data otherwise followed those described by Timmer et al. (2026). Throughout this report, when describing or referring to estimates from the annual analysis, we are referring to estimates from the modified annual analysis. We simulated all seven trends for every species represented in simulations.

We calibrated statewide average population size and annual variation based on statewide density estimates from the IMBCR annual analysis (hereafter statewide density estimates). We fixed statewide densities for simulated populations during the observation period to match statewide (posterior median) estimates exactly. We then anchored simulated trends so that the trend line intersected the average observation-period densities (details in Section 4.1.1, Appendix A). Finally, we calculated the standard deviation of observation-period population densities from the simulated trend, and simulated future-period densities assuming annual variation described by this standard deviation parameter. Because observation-period densities did not actually arise from simulated trends, observation-period densities often differed in trajectory from future-period densities. Differences between simulated and observed trends could imply changing population trajectories during long-term monitoring because such differences would mean that the overall trend across both observation and future periods did not coincide with the trend used to simulate future densities. For example, a species increasing at a rate of 3% per year during a 15-year observation period and then declining by 5% per year during a 10-year future period would have an overall trend of approximately 0% per year (about -0.1% per year, estimated as the log-linear regression slope) across the combined period, rather than the -5% per year used to simulate the future period. We therefore calculated the overall trend across both observation- and future-period densities, and treated this trend as the true effect size for evaluating statistical power (hereafter realized trend; Section 4.1.4, Appendix A). Statewide densities representing simulated populations are visualized in a series of plots contained in `results/figures/sim_trends/trend_subplots/` (see also Figure 2).

We distributed simulated statewide populations among strata and further distributed and jittered strata-level population densities to determine grid-cell level population densities based on relevant parameter estimates from the annual analysis (Sections 4.1.2 and 4.1.3, Appendix A). Strata-level densities and variability therein among grid cells are visualized in `results/figures/sim_trends/strata_subplots/no_error` and `results/figures/sim_trends/strata_subplots/with_error`.

Table 2. Baseline sampling effort in Wyoming (grid cells per year) reported as the total and within state × Bird Conservation Region (BCR) intersections. Stratum-level baseline effort is the median number of grid cells surveyed in each stratum during 2010–2024, rounded down; BCR and total values sum the stratum-level values.

BCR	Area (km^2)	n strata	n grid cells
9	119	1	2
10	165332	23	114
16	11594	4	25
17	64164	6	32
18	12258	3	16
Total	253467	37	189

Sampling scenarios

Baseline sampling

The baseline scenario for simulations matched typical (median) historical sampling effort and distribution within Wyoming over the IMBCR monitoring period leading up to this study. Although the IMBCR program began in 2008, we initiated simulations in 2010 to avoid complexities in simulation structure that would have been required to represent changes in stratification implemented prior to this year. Thus, the observation period for simulations started in 2010 and ended in 2024, the year preceding this study. Sampling effort and distribution during the observation period for all scenarios matched levels implemented in corresponding years. For the future period under the baseline scenario, we set the number of grid cells in each stratum to its median annual number of grid cells surveyed during the observation period, rounded down. Baseline statewide effort is the sum of these stratum-level medians, and baseline distribution is each stratum's share of that total (Table 2).

Alternative sampling scenarios

We simulated data under three series of alternative sampling scenarios, under which power was compared to baseline power. Again, all scenarios entailed sampling effort and distribution during the observation period that matched those actually implemented in corresponding years, and alternative scenarios only deviated in sampling effort or distribution from the baseline in future years.

The sampling effort series of scenarios (addressing Questions 1a and 1b) maintained the baseline sampling distribution among strata while varying total statewide sample effort in increments of 50 grid cells. We considered effort scenarios of -100 to +200 grid cells relative to the baseline effort (Figure 3). Additionally, following federal funding cuts in 2025, we added an alternative effort scenario of -126 grid cells, reflecting the real possibility of loss in all federal funding for IMBCR in Wyoming.

Table 3. Sampling distribution scenarios simulated for Wyoming. Each scenario favored one agency superstratum or habitat class by increasing grid cells in its strata by the stated percentage of their baseline grid cells and decreasing grid cells in all other strata by the same number of grid cells, so total effort stayed at the baseline level (189 grid cells per year). Habitat classes are represented by the strata that together comprise 95% of the class's area. Grid cells are annual totals during the future period. Figure 3 illustrates the BLM, Grassland, and Arid shrubland scenarios.

		Favored strata		Other strata	
Favored group	Increase (%)	Baseline	Scenario	Baseline	Scenario
Agency distribution scenarios					
BLM	60	54	86	135	103
Other (non-federal)	60	58	93	131	96
USFS Region 2	60	33	53	156	136
Thunder Basin National Grassland	60	10	16	179	173
USFS Region 4	60	34	54	155	135
Habitat distribution scenarios					
Conifer forest	30	130	169	59	20
Hardwood forest	60	109	174	80	15
Pine juniper	60	67	107	122	82
Dry conifer forest	60	95	152	94	37
Rangeland	60	112	179	77	10
Grassland	60	60	96	129	93
Arid shrubland	60	102	163	87	26
Riparian marsh water	30	129	168	60	21
Alpine	60	60	96	129	93

Two sampling distribution scenario series maintained baseline effort while varying how sampling was distributed among strata. Agency distribution scenarios altered baseline sampling to favor strata representing alternative jurisdictions of federal land management agencies (Questions 2a and 2b). Habitat distribution scenarios favored strata representing habitat classes defined by LANDFIRE existing vegetation types (EVT; Question 2b; see `results/LANDFIRE_classes.csv`). Most alternative distribution scenarios entailed increasing the number of grid cells in the favored class by 60% and reducing grid cells in the unfavored class by the same amount; however, for the riparian/marsh/water redistribution scenario and for the conifer forest redistribution scenario in Wyoming, there were not enough grid cells in the unfavored class, so we only increased grid cells in the favored class by 30%. We tracked effects of habitat-oriented sampling distribution on power to discern trends for two species groups, those associated and those not associated with the habitat class favored by sampling. For each habitat class, we identified an initial list of habitat associates by ranking species based on their relative abundance at survey points classified as habitat versus non-habitat, and then added to this list based on our knowledge of species ecology. Species associations with each habitat class are indicated in `results/reference/Species_list_analysis.csv`, and the number of grid cells representing each stratum under each scenario during the future period is listed in `results/reference/Sampling_scenarios.csv`. Table 3 summarizes how grid cells were distributed between favored and other strata under each distribution scenario.

Simulation approach and estimator properties

We simulated the entire IMBCR process (i.e., sampling, data collection, data analysis, and population estimation) under each population and sampling scenario for every species. Replicating simulations and summarizing across replicates allowed us to measure estimator properties. We simulated 100 replicates per scenario. Simulated count data mirrored the structure of IMBCR data analyzed during the annual analysis, and the model implemented for simulation closely followed the analysis model except additional elements needed to specify underlying processes (see above) and the observation process (Appendix A).

Statistical power

We primarily considered statistical power to discern statewide population trends to inform IMBCR sampling effort and distribution across Wyoming. We measured statistical power for 80%, 90%, and 95% credible intervals, wherein power is the proportion of replicates in which the credible interval excluded the possibility of a flat trend (i.e., non-zero % annual change) assuming the true population trend was indeed non-zero. We considered power ≥ 0.8 adequate for discerning a given trend for a given focal species under a given sampling scenario (hereafter sufficient power; Sokal and Rohlf (1995)). Since we knew the true trend, we distinguished between "accurate" power and "inaccurate" power, i.e., the proportion of replicates when a trend was discerned in the same or opposite direction, respectively, as the true trend. We focused on accurate power to inform sampling design, so hereafter, "power" refers to accurate power. Having corrected bias (see below), inaccurate power was low and only appeared under scenarios when the realized trend was essentially flat (i.e., close to 0% annual change). We therefore ignored inaccurate power except when discussing bias (see below). Although we focus on discernment of statewide population trends in this report, we did generate and store power estimates for discerning trends and capable of informing sampling levels for individual strata and federal agency-level superstrata (see `results/Sum_output_agency.csv`, `results/Sum_output_strata.csv`, and `results/figures/effort_scns/Figure_power_[80,90,95]CI_stratum.csv`).

Bias

Having simulated data from known populations, we compared estimates with known population parameters to assess estimation accuracy and bias. Considering statistical power without regard to estimator accuracy could yield misleading conclusions for sampling design. Distinguishing between accurate and inaccurate power guarded against egregiously misleading conclusions. Additionally, measuring accuracy and bias can provide more information and context for interpreting statistical power. We calculated bias as the deviation of trend estimates from the realized trend (Appendix A, Section 4.1.4) rather than the nominal simulated trend, since observation-period densities were fixed to their actual historical values rather than generated by the simulated trend itself. We did measure substantial bias in density estimates and some bias in trend estimates, and we were unable

to determine the extent to which observed bias represented actual estimator properties versus artifacts of our simulation approach (see Results). We therefore corrected trend estimation bias by subtracting estimated bias from trend estimates before deriving estimates of power. We derived inference of statistical power and conclusions for sampling design based primarily on bias-corrected power estimates, but we also provide uncorrected power estimates in `results/bias_uncorrected/` for comparison. We consider the implications of bias for our conclusions, and we provide additional details on how we measured estimator properties in Section 6, Appendix A.

Results

Power relationships

Sampling effort

We estimated adequate power (≥ 0.8) to discern any statewide trend with an 80% CI under any sampling scenario considered in our simulations for 63 of 80 species (43 of 58 SGCN) in Wyoming (Table 1). We estimated adequate power for discerning moderate to strong trends (ca. 2–6% annual change) for approximately 19–85% of species, and weak trends (0.75–2.25% annual change) for approximately 2–8% of species (`results/figures/effort_scns/Figure_power_[80,90,95]CI_statewide_sum.csv`).

We saw substantial losses in species with adequate power with decreasing sampling effort below historical levels (Figure 4, Figure 5; `results/figures/effort_scns/Figure_power_[80,90,95]CI_statewide_sum.csv`). Dropping sampling effort in increments of 50 grid cells below historical levels resulted in a loss of up to 7 species with adequate power in Wyoming. The largest set of species lost with an incremental drop in sampling effort was 7 species (including 5 SGCN; American Pipit, Baird's Sparrow, Black Rosy-Finch, Common Yellowthroat, Northern Harrier, Olive-sided Flycatcher, and Williamson's Sapsucker) lost when dropping from 189 to 139 grid cells under 5% annual population decline scenarios discerned with 80% CIs (Figure 5; `results/Spp_gained_w_sample_size.csv`).

We saw relatively modest gains in species with adequate power when increasing sampling effort above historical levels (Figure 4, Figure 5; `results/figures/effort_scns/Figure_power_[80,90,95]CI_statewide_sum.csv`). Increasing sampling effort in increments of 50 grid cells above historical levels resulted in gains of up to 3 species with adequate power. The largest set of species gained with an incremental increase in sampling effort was 3 species (including 0 SGCN). With a 3% annual declining trend and 80% credible interval, we gained Lark Bunting, Western Kingbird, and Wilson's Warbler when increasing from 189 to 239 grid cells, although the gain for Western Kingbird was small (power increased by 0.04, compared with 0.07 for Lark Bunting and 0.11 for Wilson's Warbler) (Figure 5; `results/Spp_gained_w_sample_size.csv`).

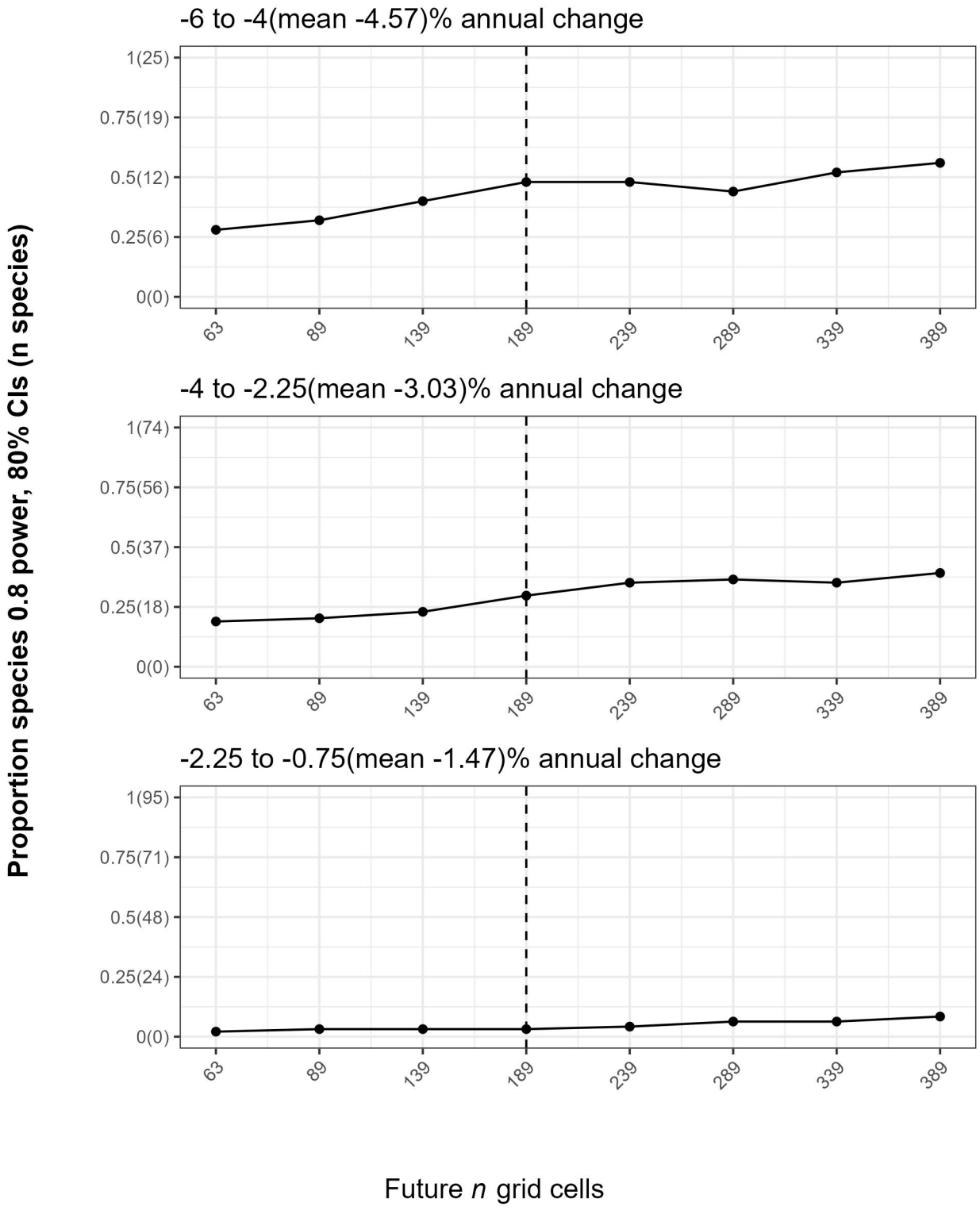


Figure 4. Proportion of Wyoming species of interest with accurate power ≥ 0.8 to discern declining statewide trends using an 80% credible interval, for each of three simulated annual decline magnitudes (1.5%, 3%, and 5%), under alternative levels of sampling effort for future (2025–2034) monitoring. Vertical dashed lines mark baseline (historical) sampling effort.



Figure 5. Species for which we achieved ≥ 0.8 power to discern declining statewide trends under alternative sampling effort scenarios using an 80% credible interval. Only the 35 species for which we achieved ≥ 0.8 power under a declining trend scenario within the effort sampling scenario series in Wyoming are represented here. Circles indicate where power reached ≥ 0.8 for given species at or below the sampling effort for that scenario. Circle size and color indicate the magnitude of the simulated trend (1.5%, 3%, or 5% annual decline; i.e., the effect size). Species are ordered alphabetically; dashed vertical line marks baseline (historical) sampling effort. Note: in some cases, power estimates declined slightly from lower to higher sample sizes, but we attributed these minor declines to sampling error ($n = 100$ simulations per scenario), and therefore ignored them here.

Sampling distribution

We saw no major gains or losses in the proportion of species with adequate power with sampling redistribution to agency-specific strata while maintaining total baseline sampling effort (Figure 6; `results/figures/agency_distn_scns/Figure_power_[80,90,95]CI_statewide_sum.jpg`). Under future-period population trends of 1.5% or 3% annual decline and power discerned with 80% CIs, net gains or losses in species with adequate power were never more than one species for any single redistribution scenario. Using an 80% CI to discern trends, the largest change in the set of species with adequate power in any single scenario was under redistribution favoring non-federal ("Other") lands at a 3% annual decline scenario: Lark Bunting, Western Kingbird, and Wilson's Warbler were gained (including 0 SGCN), while American Three-toed Woodpecker and Steller's Jay were lost (including 0 SGCN) (Figure 7; `results/Spp_gains_losses_by_agncy_distr_scn.csv`). The underlying changes in power were small for most of these species: power increased by only 0.03–0.04 relative to baseline for the three species gained and decreased by 0.02 for Steller's Jay, whereas power for American Three-toed Woodpecker declined by 0.06. Additionally, under a 1.5% annual decline scenario, Dark-eyed Junco gained adequate power in four of the five agency redistribution scenarios (Figure 7), although power increased by 0.05 or more relative to baseline in only two of them (those favoring non-federal lands and USFS Region 4). These gains likely reflect that Dark-eyed Junco had power just below the threshold under baseline effort (0.79 with an 80% CI and a 1.5% decline), combined with the concentration of its statewide abundance in a few sparsely sampled, high-elevation strata (four BCR 10 strata held roughly 55% of its estimated statewide abundance but only 20 of 189 baseline grid cells): scenarios that added grid cells to these strata (e.g., Alpine, USFS Region 4, conifer forest, and riparian/marsh/water redistribution) raised power above 0.8, whereas scenarios that removed cells from them (e.g., rangeland and dry conifer forest redistribution) lowered it. Because baseline power was so close to the threshold and simulation error is appreciable (100 replicates per scenario), small and partly random shifts could also have moved the species across the threshold in other scenarios. We saw no gains or losses in species with adequate power when discerning power with 90% or 95% CIs (`results/Spp_gains_losses_by_agncy_distr_scn.csv`).

We saw predominantly positive net changes in the number of species with adequate power with sampling redistribution to strata representing particular habitat classes while maintaining total baseline sampling effort (Figure 8; `results/figures/habitat_distn_scns/Figure_power_[80,90,95]CI_statewide_sum[habitatclass].jpg`, `results/Spp_gains_losses_by_habitat_distr_scn.csv`). Under future-period population trends of 1.5% or 3% annual decline and power discerned with 80% CIs, redistribution favoring a single habitat class never resulted in a net loss of more than 1 species, while net gains reached as many as 2 species. In particular, under a 1.5% decline, we saw no net losses at all and only gains of up to 2 species (Figure 8). Using an 80% CI, the largest net gains, 2 species, occurred with redistribution favoring conifer forest, pine-juniper, or alpine strata under 3% decline scenarios. Conifer forest redistribution gained the conifer-associated Wilson's Warbler along with Western Kingbird (0 SGCN); pine-juniper redistribution gained Lark Bunting, Western Kingbird, and Wilson's Warbler (0 SGCN) while

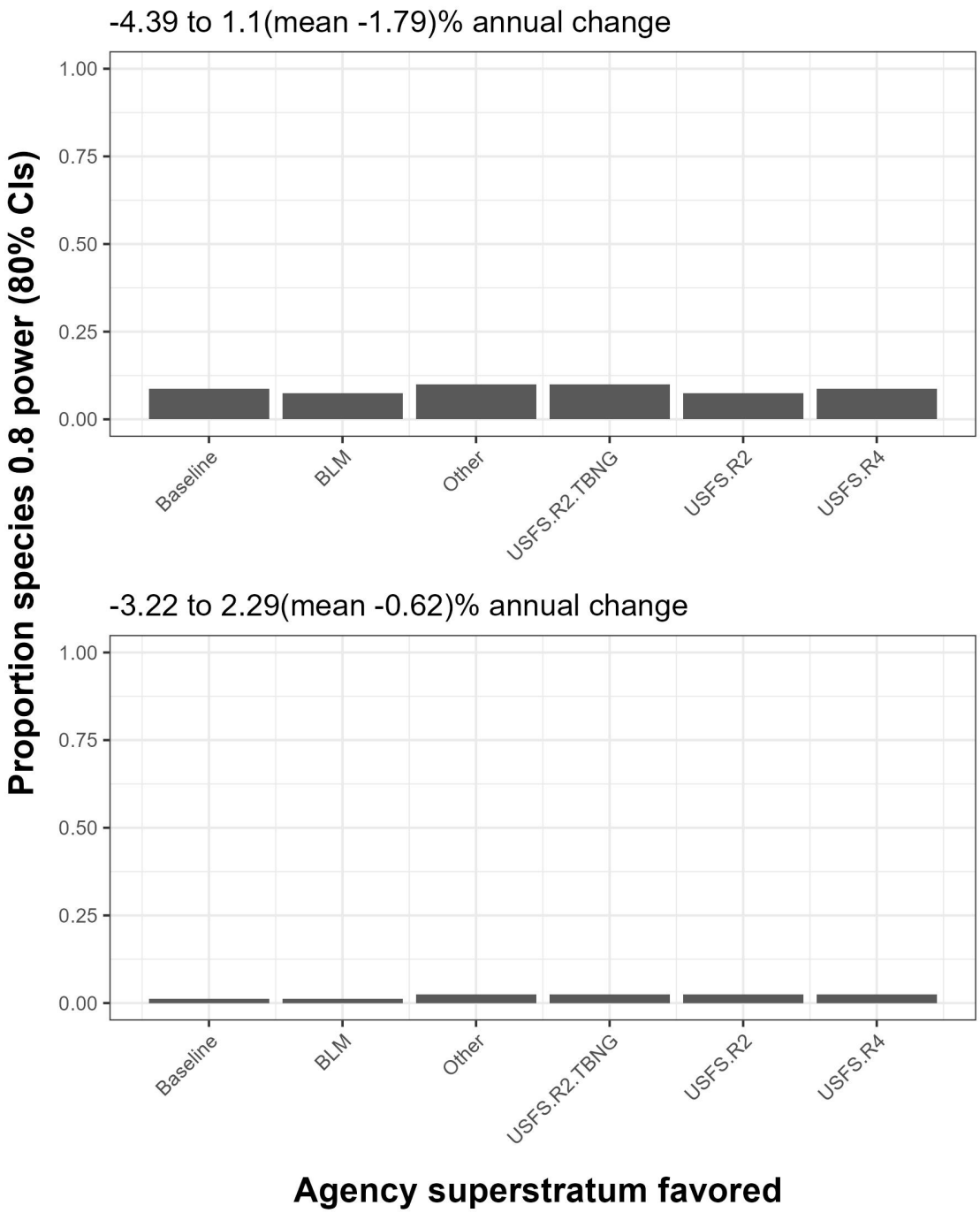


Figure 6. Proportion of Wyoming species of interest with accurate power ≥ 0.8 to discern declining statewide trends using an 80% credible interval under alternative agency distribution scenarios for each of two simulated annual declines (3% (top panel) and 1.5% (bottom panel)) applied during future years (2025–2034). The range and mean of realized trends across the entire monitoring period (2010–2034) are listed above each panel. Agency superstrata favored (x-axis): BLM = Bureau of Land Management; Other = non-federal lands; USFS.R2 = U.S. Forest Service Region 2; USFS.R2.TBNG = Thunder Basin National Grassland (Region 2); USFS.R4 = U.S. Forest Service Region 4.

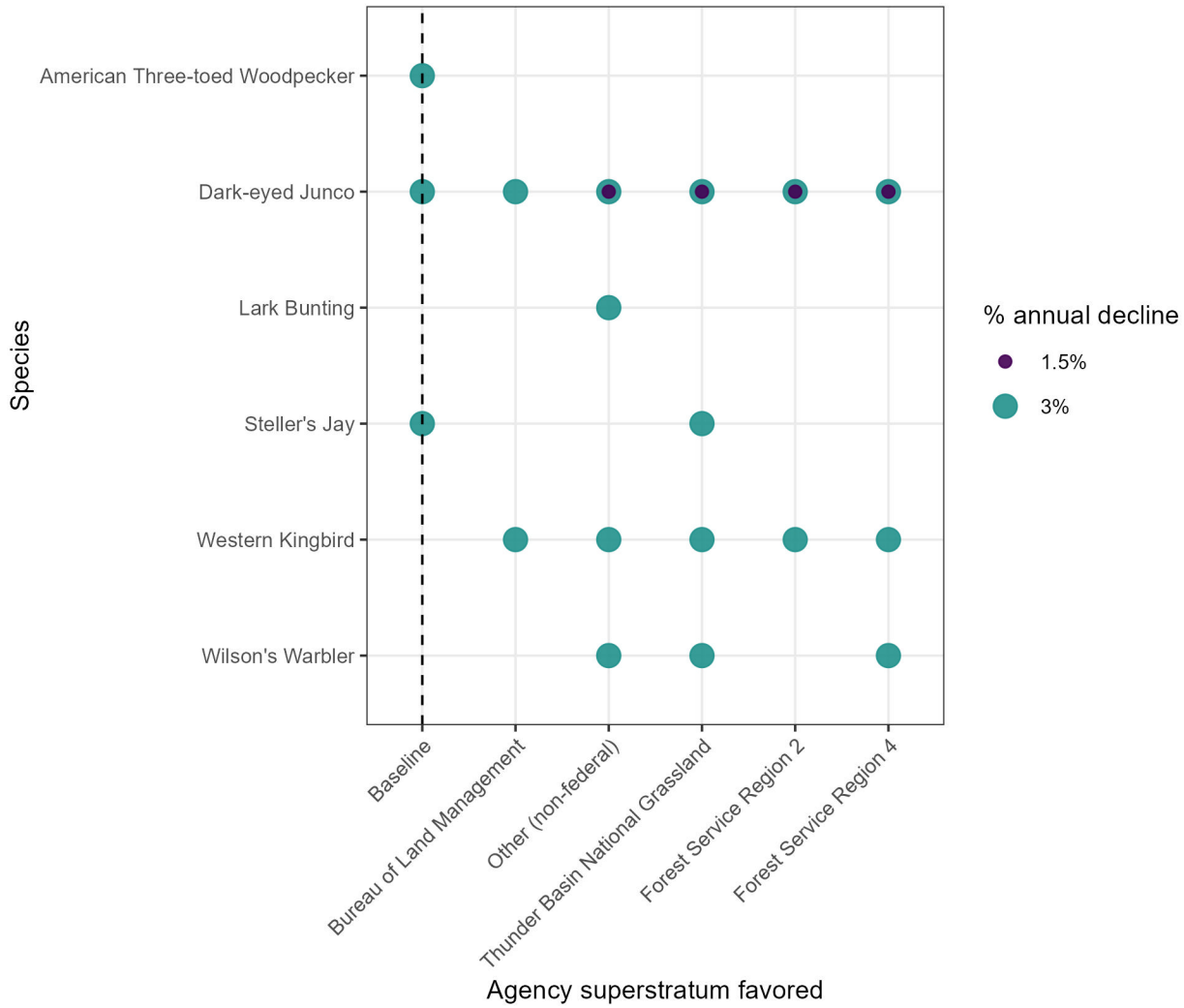


Figure 7. Species-specific accurate power ≥ 0.8 to discern declining statewide trends using an 80% credible interval, under alternative agency sampling distribution scenarios for future (2025–2034) monitoring. Only species for which power differed from the baseline distribution under at least one scenario are shown; species that maintained consistent power (either always or never ≥ 0.8) across all agency distribution scenarios considered are omitted (Figure 5). Circles indicate where power reached ≥ 0.8; circle size and color indicate the magnitude of the simulated trend (1.5% or 3% annual decline; i.e., the effect size). Species are ordered alphabetically; dashed vertical line marks the baseline distribution.

losing American Three-toed Woodpecker (0 SGCN); and alpine redistribution gained Western Kingbird and Wilson's Warbler (0 SGCN) (Figure 9). The largest net losses, 1 species each, occurred with redistribution favoring hardwood forest or arid shrubland strata under a 3% decline, both driven by losses of American Three-toed Woodpecker and Steller's Jay (neither SGCN) only partly offset by a gain of Savannah Sparrow or Western Kingbird, respectively (Figure 9; `results/Spp_gains_losses_by_habitat_distr_scn.csv`). We saw far fewer changes in species with adequate power when discerning power with 90% or 95% CIs: at a 90% CI, only Chipping Sparrow was lost, and only under a 1.5% decline with redistribution favoring hardwood or dry conifer forest strata. At a 95% CI, only Clark's Nutcracker and Hermit Thrush were lost (1 SGCN), under a 3% decline with redistribution favoring dry conifer forest or rangeland strata; no gains were observed at either CI (`results/Spp_gains_losses_by_habitat_distr_scn.csv`).

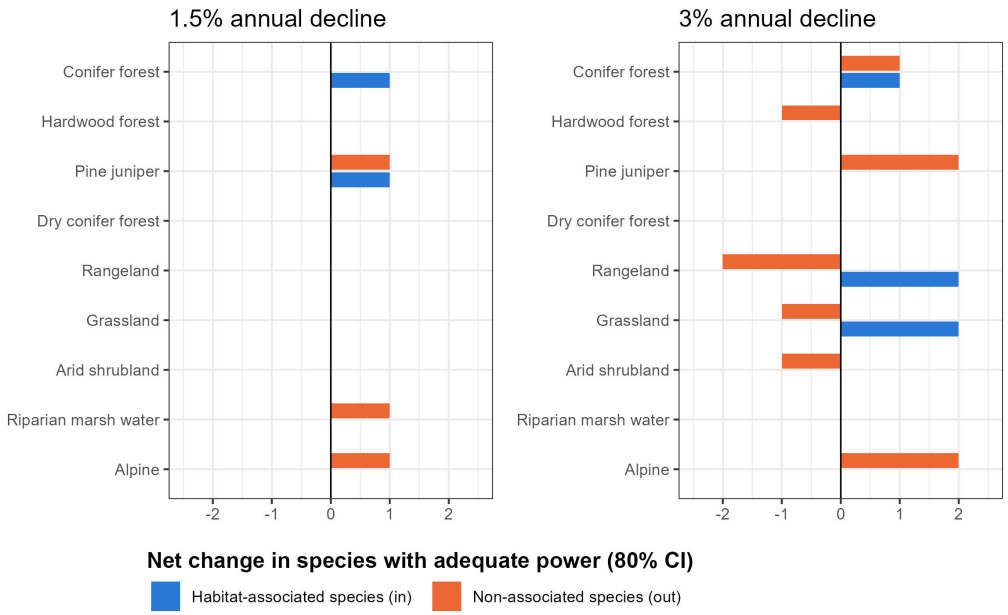


Figure 8. Net change (species gained minus species lost) in the number of Wyoming species with accurate power ≥ 0.8 to discern declining statewide trends using an 80% credible interval, under alternative habitat sampling distribution scenarios for each of two simulated annual declines (1.5% (left panel) and 3% (right panel)) applied during future (2025–2034) monitoring. Species are grouped by whether they are associated ("in") or not associated ("out") with the favored habitat class (see Table 1).

Bias

We found notable bias in density and trend estimates. Statewide trend estimates did not exhibit clear bias on average (median bias [5th, 95th percentiles] = 0 [-2, 2] % annual change; n = 6,704 scenarios), but trend estimates were biased in opposite directions across trend scenarios (Figure 10). Density estimates tended to be negatively biased (median bias [5th, 95th percentiles] = -0.2 [-8.38, 0.01]; n

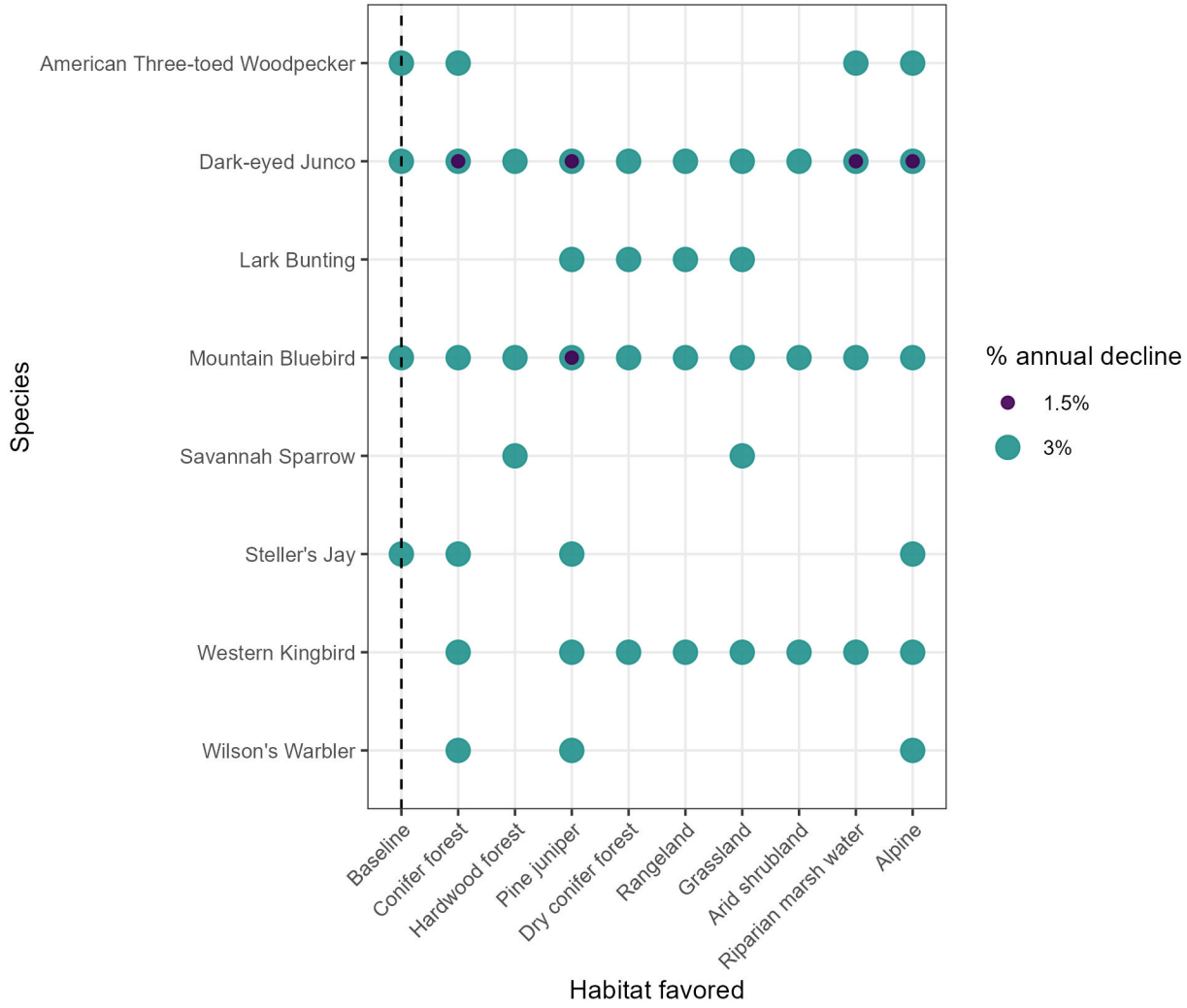


Figure 9. Species-specific accurate power ≥ 0.8 to discern declining statewide trends using an 80% credible interval, under alternative habitat sampling distribution scenarios for future (2025–2034) monitoring. Only species for which power differed from the baseline distribution under at least one habitat scenario are shown; species that maintained consistent power (either always or never ≥ 0.8) across all habitat distribution scenarios considered are omitted (Figure 5). Circles indicate where power reached ≥ 0.8; circle size and color indicate the magnitude of the simulated trend (1.5% or 3% annual decline; i.e., the effect size). Species are ordered alphabetically; dashed vertical line marks the baseline distribution.

= 91,780 species × trend scenario × sampling scenario × stratum combinations), and increasingly so with increasing (true) population density (hereafter D; Pearson's r = -0.96). Because density estimation bias became more negative with increasing D, density was underestimated more severely in higher-density portions of any population trajectory, compressing the estimated trend toward zero. Attenuation of trend estimates toward zero explained the opposing biases with strongly positive versus negative trends, and less bias with weak or flat trends (Figure 10). Density estimation bias is reported in `results/Sum_density.csv` and visualized in `results/figures/spp_densities/` and `results/figures/sim_trends/strata_subplots/sim_dens/`. Statewide trend estimation bias is further reported in `results/bias_uncorrected/Sum_output_state.csv` and visualized in `results/bias_uncorrected/figures/effort_scns/spp_trend/`.

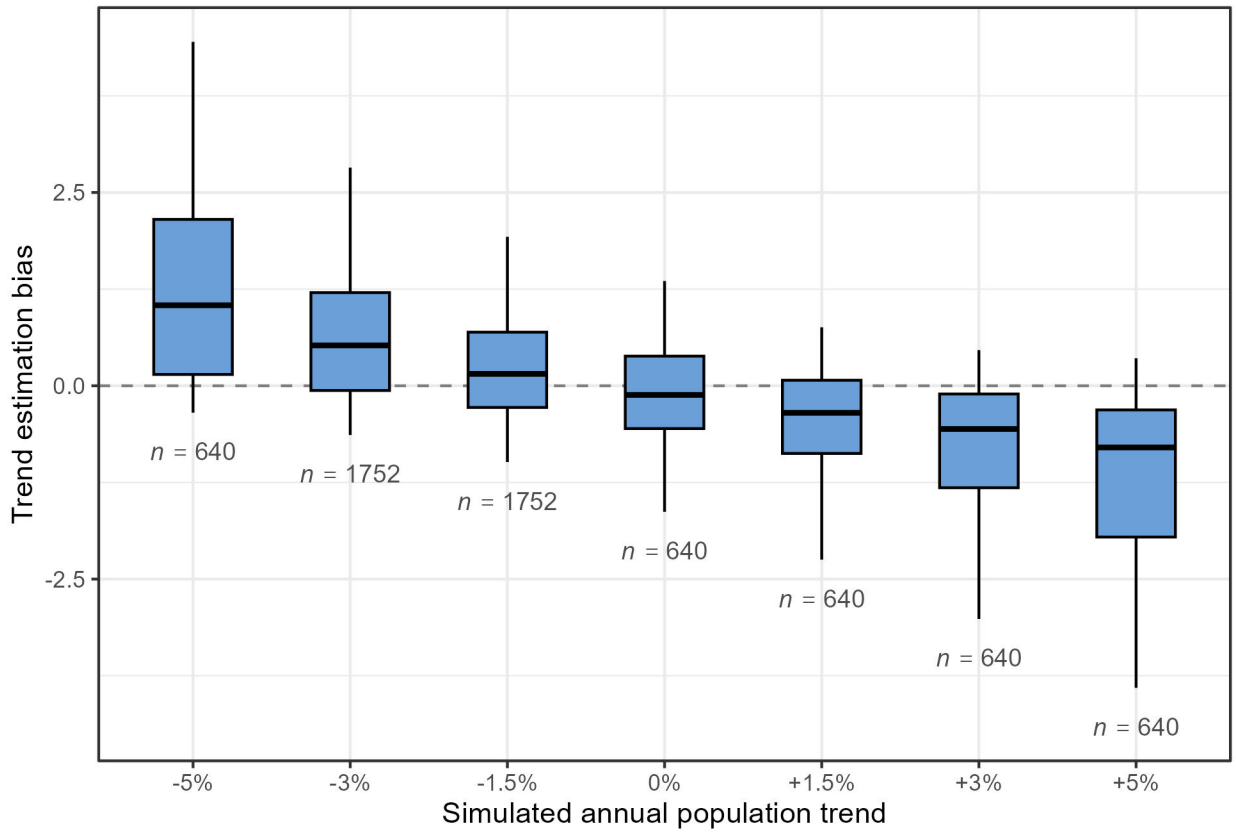


Figure 10. Trend estimation bias for each simulated annual population trend (x-axis) in Wyoming, pooled across all species and sampling scenarios. Bias (y-axis, in percentage points annual change) is the difference between estimated and realized (true) statewide trends (realized trend defined in Appendix A, Section 4.1.4). Box, center line, and whiskers show the interquartile range, median, and 5th–95th percentiles, respectively, of bias values across all species × sampling-scenario combinations simulated at that trend. n provides the count of species × sampling-scenario combinations represented in each box.

This bias has consequences for species-level conclusions about statistical power. Of 80 focal species, 17 (21%) would not have met the sufficient-power criterion (accurate power $\geq$ 0.8 in at least

one scenario considered) without bias correction (Table 1); bias correction increased rather than decreased this classification for every such species, consistent with the attenuation described above. At the level of individual scenarios, accurate power estimates (80% credible interval) shifted by 0.06 on average with bias correction, and by ≥ 0.2 in 17% of species $\times$ scenario combinations. Uncorrected power estimates are provided in `results/bias_uncorrected/` for comparison.

Discussion

Within sampling scenarios considered here, total statewide sampling effort had greater influence on the number of species of interest (including SGCN) with adequate power to detect statewide trends with IMBCR than did redistribution of sampling among strata. The historical (baseline) level of sampling effort appears nearly optimal, with considerable loss of power under scenarios of reduced effort and fewer gains for equivalent increases. Reducing sampling effort below historical levels would clearly compromise statistical power, particularly beyond reductions of more than 50 grid cells statewide, which could occur if contributions from one or two funding partners were discontinued. Increasing sampling effort above historical levels could benefit power, but these benefits would be relatively incremental compared to the magnitude of losses expected with reduced sampling effort. The greater cost of decreasing versus benefit with increasing sampling effort suggests historical (baseline) effort may be near an inflection point beyond which returns for increasing the number of species for which we effectively monitor statewide trend diminish with increased sampling effort. Nevertheless, increasing overall sampling effort could broaden IMBCR coverage to include more species (e.g., Lark Bunting, Wilson's Warbler, and Dark-eyed Junco), as well as benefit other monitoring objectives such as discerning strata-level trends and providing reference data for evaluating management.

We were less able to influence statistical power by redistributing sampling among strata. In particular, varying relative support for IMBCR among federal agencies would apparently not tremendously compromise or benefit the number of species with adequate power assuming overall sampling effort is maintained, although some shuffling of species with adequate power would be expected. Habitat-focused redistribution showed a more favorable pattern: redistribution favoring strata representing particular habitat classes could benefit power for a few habitat-associated species (e.g., Lark Bunting, Wilson's Warbler, and Dark-eyed Junco). For Lark Bunting, for example, redistribution toward grassland or rangeland strata raised power (from 0.77 to 0.84 and 0.89, respectively, under a 3% annual decline with an 80% CI) by about as much as adding 50 to 150 grid cells (power of 0.84–0.88). Power was lost for other species only rarely, and never for more than one species per scenario (e.g., American Three-toed Woodpecker and Steller's Jay). In short, while redistribution of sampling among strata cannot make up for loss of sampling effort, our results identify species that could benefit from habitat-focused redistribution with comparatively little loss of other species. Therefore, redistribution is an option worth considering alongside maintenance of existing sampling effort. Additionally, because we considered scenarios with increasing effort and allocation to strata

separately, it is possible that further gains could be achieved by increasing effort in a subset of strata of interest (e.g., grasslands).

Monitoring recommendations

Above all, we recommend prioritizing maintenance of historical statewide sampling effort to sustain the overall value of IMBCR for monitoring SGCN and species of conservation concern for federal agencies. Given recent declines in funding support in 2025–2026, this would require increasing effort by roughly 55–65 grid cells per year to restore the baseline level of 189 grid cells per year. Without increasing effort over baseline levels, we recommend concentrating state-funded surveys in grassland-dominated strata to improve power for Lark Bunting, a grassland species of high conservation concern. Additional funds available beyond the amount required to maintain baseline effort could be used for "overlay projects" (supplemental strata defined for particular objectives, such as monitoring within areas subject to management action; Timmer et al. (2026)) to answer priority questions on the effects of management, or to increase baseline effort in specific areas of interest to funding partners, including individual strata (e.g., Tribal lands, a BLM field office, a USFS National Forest or Grassland, a National Park) or superstrata (e.g., all BLM lands, all USFS lands).

Study limitations and future directions

Simulating realistic datasets under the stratified design of IMBCR proved more challenging than expected. This resulted in some unresolved biases in abundance and trends that limited our confidence in making management recommendations based on the results of this study. We found that increasing negative bias in density estimates with increasing population density directly explains the pattern of trend estimation bias we observed: because density is more severely underestimated in higher-density portions of a population trajectory, estimated trends are compressed toward zero relative to the realized trend, with the degree of compression scaling with the magnitude of the true trend (Figure 10). We did not expect observed estimation biases based on existing theory or patterns described in the literature, although it is broadly consistent with shrinkage toward the population mean, a well-documented feature of hierarchical models. We have not formally tested this explanation, but alternative model structures or priors that reduce shrinkage would be worth exploring in future research. Regardless, until we have identified and can eliminate it, uncorrected power estimates could represent reality, so we provide uncorrected estimates in `results/bias_uncorrected/` for comparison. For now, power estimates and patterns that differ from those without bias correction should be interpreted and applied with relative caution.

Several study limitations suggest potential avenues for future research. We only considered power for discerning statewide population trends. When selecting from levels of sampling effort and distribution that minimally influence power reported here, power for discerning agency-level or strata-level trends may be additionally informative (`results/Sum_output_agency.csv`, `results/Sum_output_`

`strata.csv`, and `results/figures/effort_scns/Figure_power_[80,90,95]CI_stratum.jpg`). For example, federal partners might be interested in understanding power for priority species within the lands they manage, rather than statewide. Simulations here assumed invariant sampling effort and distribution over a 10-year future period, whereas fluctuations in funding for IMBCR sampling may in reality occur over shorter timeframes. Evaluating how precision in density estimates (in addition to power to discern trend) varies with alternative levels of sampling effort and distribution may more clearly inform year-to-year sampling decisions; although not described in this report, we did generate data describing density estimator precision (`results/Sum_density.csv`). Thus in the future, we could mine existing simulations to relate density precision with sampling effort and distribution, or rerun simulations (perhaps after better understanding and resolving density estimation bias) and collect additional metrics of density precision (e.g., coefficient of variation).

Scenarios considered here do not represent all conceivable sampling options available to WGFD, but rather illuminate patterns relevant for a range of sampling decisions. We designed sampling distribution scenarios to be separate from sampling effort scenarios so that we could distinguish the independent relationships of effort and distribution with power, but available sampling options could involve adjusting both. In particular, we simulated agency and habitat redistribution only at baseline effort, so we did not evaluate whether combining added effort with redistribution toward particular habitat classes or agencies would gain power for additional species or maintain it for species of concern. For example, adding sampling effort to strata representing particular habitat classes could boost power for habitat-associated species without compromising power for other species. Moreover, an unmitigated drop in effort within strata managed by a particular federal agency could be particularly harmful to power for species that benefitted from favoring that agency in our simulations. Having stored and documented all code for implementing simulations described here in a git repository, we have facilitated further simulations relevant to particular sampling decisions.

References

Andersen, E. M., and R. J. Steidl. 2020. Power to detect trends in abundance within a distance sampling framework. Journal of Applied Ecology 57:344–353.

Guillera-Arroita, G., and J. J. Lahoz-Monfort. 2012. Designing studies to detect differences in species occupancy: Power analysis under imperfect detection. Methods in Ecology and Evolution 3:860–869.

Latif, Q. S. 2021. Power analysis and sampling recommendations for breeding bird monitoring at Camp Guernsey, Wyoming: Report. Bird Conservancy of the Rockies, Brighton, CO, USA.

Latif, Q. S., Z. P. Wallace, L. G. Rossi, J. M. Timmer, and C. E. Latimer. 2026. Simulation-based power analysis and sampling recommendations for IMBCR in colorado. Bird Conservancy of the Rockies, Brighton, Colorado, USA.

MacKenzie, D. I., J. D. Nichols, G. B. Lachman, S. Droege, J. A. Royle, and C. A. Langtimm. 2002. Estimating site occupancy rates when detection probabilities are less than one. Ecology

83:2248–2255.

Mackenzie, D. I., and J. A. Royle. 2005. Designing occupancy studies: General advice and allocating survey effort. Journal of Applied Ecology 42:1105–1114.

McLaren, M. F., C. M. White, N. J. Van Lanen, J. J. Birek, M. C. Smith, and J. Reese. 2025. Integrated Monitoring in Bird Conservation Regions (IMBCR): Field protocol for spatially balanced sampling of land bird populations.

NABCI Monitoring Subcommittee. 2007. Opportunities for improving avian monitoring. U.S. North American Bird Conservation Initiative, Arlington, VA.

Pavlacky, D. C., P. M. Lukacs, J. A. Blakesley, R. C. Skorkowsky, D. S. Klute, B. A. Hahn, V. J. Dreitz, T. L. George, and D. J. Hanni. 2017. A statistically rigorous sampling design to integrate avian monitoring and management within Bird Conservation Regions. PLOS ONE 12:e0185924.

Rocky Mountain Avian Data Center 2.0. 2024. RMADC 2.0: A portal for avian information from the IMBCR program [web application]. Bird Conservancy of the Rockies, Brighton, Colorado.

Sokal, R. R., and J. F. Rohlf. 1995. Biometry. Third. W. H. Freeman; Company, New York, NY.

Stevens, D. L., and A. R. Olsen. 2004. Spatially balanced sampling of natural resources. Journal of the American Statistical Association 99:262–278.

Timmer, J. M., J. A. Reese, M. F. McLaren, M. C. Smith, T. C. Walker, C. M. White, Q. S. Latif, D. C. Pavlacky, and R. A. Sparks. 2026. Integrated monitoring in bird conservation regions (IMBCR): 2025 field season report. Bird Conservancy of the Rockies, Brighton, Colorado, USA.

Wyoming Game and Fish Department. 2017. Wyoming state wildlife action plan. Wyoming Game; Fish Department, Cheyenne, Wyoming, USA.

Appendices

Appendix A — Simulation and analysis methods

The following pages describe the detailed simulation and analysis methods summarized in the Methods section above.

Appendix A: Simulation and analysis methods

1 Overview

The simulation process consisted of 3 phases:

1. **Scenario construction** - formulate trend and sampling scenarios reflecting known species ecology and available sampling options of interest to state wildlife agencies.
2. **Data simulation** - simulate data under alternative trend and sampling scenarios formulated in phase 1.
3. **Data analysis** - analyze data simulated in phase 2 and estimate statistical power and other estimator properties (e.g., bias and coverage).

We first describe our analysis model, including ecological and observation process sub-models. Referencing the analysis model, we then describe each of these phases of the simulation process.

2 Indices

l - Bird Conservation Regions with max L.

i - strata with max I, which is the number of strata where the species was ever detected; since strata are nested with Bird Conservation Regions, an index i implies indexing by l.

j - grid cells with max J; since grid cells are nested within strata, which in turn are nested with Bird Conservation Regions, an index j implies indexing by i and l, although we often included both i and j in our notation for clarity.

k - points within a grid cell with general max $K = 16$ and unit-specific max $K_{[s]}$ points surveyed in grid cell j

d - distance bins with max $d_{[max]} = 10$

$d_{[mid]}$, $d_{[low]}$, and $d_{[high]}$ are the distance mid-point, lower bound, and upper bound for distance bin d. $d_{[max,high]}$ is the upper bound for the furthest distance bin (i.e., the radius of the entire point-level plot).

r – 2-min time removal bins within the 6-min survey with max $R = 3$

t – years with max T

g – posterior samples with max G

x - simulations with max X per scenario

3 Analysis model

Our analysis model was essentially the same as the model implemented for the IMBCR annual analysis, which is described in detail in the annual report (Appendix D, Timmer et al. 2026). We constructed population scenarios for simulations (phase 1) based on estimates produced by or derived from the annual analysis. We analyzed simulated data (phase 3) using a version of the annual analysis model modified to approximate analysis within a focal region (i.e., Colorado or Wyoming) within a context of program-wide analysis and estimation. In particular, we used informed priors in place of data collected outside the focal region but not explicitly represented in simulations. We describe here our modified version of the model while noting how and why this version deviates from the original version.

3.1 Ecological process

The ecological process model includes two sub-models, one quantifying species occupancy of grid cells and a second quantifying abundance at occupied grid cells. We model the species occupancy of a grid cell as

$$z_{ijt} \sim Bernoulli(\psi_{it}) \tag{1}$$

and

$$logit(\psi_{it}) \sim Normal(\mu_{[\psi],t}, \sigma^2_{[\psi],t}), \tag{2}$$

where ψ_{it} is the probability of species occupancy of a grid cell in stratum i in year t, z_{ijt} is the latent occupancy state of grid cell j in stratum i during year t, and $\mu_{[\psi],t}$ and $\sigma^2_{[\psi],t}$ are year-specific mean and variance hyper-parameters. We exclude data for all strata in which the species was never detected (approximately conditioning occupancy on being within the species range). IMBCR surveyors record detections of independent clusters, whereby a cluster is ≥ 1 individual. Usually, clusters consist of a single individual, but individuals detected together are recorded as a single cluster (e.g., a breeding pair moving together or somehow behaviorally associated so that detecting pair members cannot be considered independent events). Thus, we model density and abundance of independent clusters, and then multiply by mean cluster size to recover population density (i.e., density of individuals). We model abundance of clusters within $d_{[max,high]}$ of points within an occupied grid cell as

$$N_{[c],ijt} \sim Poisson(\lambda_{[N],ijt} \times z_{ijt}) \tag{3}$$

and

$$log(\lambda_{[N],ijt}) = \alpha_{it} + \varepsilon_{jt}. \tag{4}$$

where α_{it} and ε_{jt} are stratum- and grid-cell-specific random effects, respectively, and α_{it} is also subject to a fixed effect of year:

$$\alpha_{it} \sim Normal(\mu_{[\alpha],t}, \sigma^2_{[\alpha],t}) \tag{5}$$

and

$$\varepsilon_{jt} \sim Normal(0, \sigma^2_{[\varepsilon]}). \tag{6}$$

3.2 Observation process

We model the sum of observed counts (of independent clusters of individuals) across all points surveyed within a grid cell (n_{ijt}) as

$$n_{ijt} \sim Binomial\Big(N_{[c],ijt}, p_{[a],tl} \times p_{[p],t} \times \frac{K_{[s],ijt}}{K}\Big), \tag{7}$$

where $p_{[a],tl}$ is a year- and BCR-specific availability component of detection probability, $p_{[p],t}$ is a year-specific perceptibility component of detection probability, and $K_{[s],ijt}$ / K is survey effort. Detection components can be expressed as the sum of probability vectors:

$$p_{[a],tl} = \sum_{r=1}^{R} \pi_{[a],tlr} \tag{8}$$

and

$$p_{[p],tl} = \sum_{d=1}^{d_{max}} \pi_{[p],tld}, \tag{9}$$

where $\pi_{[a],tlr}$ and $\pi_{[p],tld}$ are detection probabilities within time removal and distance bins (hereafter bin probabilities), respectively. We model the distribution of counted clusters among time removal and distance bins, respectively, as

$$\mathbf{y}_{\mathbf{[a],ijt}} \sim Multinomial\Big(n_{ijt}, \boldsymbol{\pi}^{\mathbf{[c]}}_{\mathbf{[a],tl}}\Big) \tag{10}$$

and

$$\mathbf{y}_{\mathbf{[p],ijt}} \sim Multinomial\Big(n_{ijt}, \boldsymbol{\pi}^{\mathbf{[c]}}_{\mathbf{[p],tl}}\Big), \tag{11}$$

where $\mathbf{y}_{\mathbf{[a],ijt}}$ and $\mathbf{y}_{\mathbf{[p],ijt}}$ are vectors of counts within time removal and distance bins. Bin probabilities for availability assume constant availability across the survey period,

$$\pi_{[a],trl} = p_{[ar],tl}(1 - p_{[ar],tl})^{r-1}, \tag{12}$$

where $p_{[ar],tl}$ is the availability for a single 2-min time removal bin. We allowed availability to vary according to a year- and BCR- specific random effect:

$$logit(p_{[ar],tl}) \sim Normal(\mu_{[p_{ar}]}, \sigma^2_{[p_{ar}]}). \tag{13}$$

Bin probabilities for perceptibility accounted for increased bin area for bins further from the surveyor.

$$\pi_{[p],td} = \frac{p_{[pd],td} A_d}{\sum_{d=1}^{d_{[max]}} A_d}, \text{ and} \tag{14}$$

where $p_{[pd],td}$ is the perceptibility within distance bin d in year t, and A_d is the area of distance bin d. Multinomial cell probabilites for modeling $\mathbf{y}_{\mathbf{[a],ijt}}$ and $\mathbf{y}_{\mathbf{[p],ijt}}$ represent bin probabilites scaled to sum to 1:

$$\pi^{[c]}_{[a],trl} = \pi_{[a],trl} \; / \; p_{[a],tl}, \tag{15}$$

and

$$\pi^{[c]}_{[p],td} = \pi_{[p],td} \; / \; p_{[p],t}. \tag{16}$$

We model $p_{[pd],td}$ using one of two possible perceptibility models: 1) a half-normal or 2) a hazard rate model. For the half-normal model, we calculated $p_{[pd],d}$ for each distance class as:

$$p_{[pd],d} = \frac{2\pi \int_{c=d_{[low]}}^{c=d_{[high]}} exp\left(-\left(\frac{c^2}{2\sigma^2_{[HN]}}\right)\right) c \; dc}{A_d}, \tag{17}$$

where $d_{[low]}$ and $d_{[high]}$ are the bounds for distance bin d and $\sigma_{[HN]}$ is the half-normal shape parameter. Because of the lack of an analytical solution to the integral of the hazard rate function, we calculated $p_{[pd],d}$ at the midpoint, $d_{[mid]}$, of each distance class:

$$p_{[pd],d} = 1 - exp\left(-\left(\frac{d_{[mid]}}{h}\right)^b\right), \tag{18}$$

where h and b are estimated parameters for the hazard function.

3.3 Priors

For computational tractability, we did not explicitly simulate data across the entire IMBCR programmatic footprint even though we wanted to represent analysis of all available data when quantifying power and estimator properties within the focal region (i.e., Colorado or Wyoming). Rather, we used informed priors for grid cell error and detectability parameters to approximately represent information entering the analysis from outside the focal region. Initially, we constructed informed priors for all parameters, but informed priors for occupancy and abundance restricted simulated trend estimates, resulting in biased trend estimates and consequently unrealistic power curves. We therefore used the same uninformed priors for estimating strata-level occupancy and abundance as is used for the annual analysis. Thus, the priors for mean stratum-level occupancy (Equation 2) and abundance (Equation 5) were

$$\mu_{[\psi],t} \sim Normal(0, 1.5), \tag{19}$$

$$\sigma_{[\psi],t} \sim gamma(1, 1), \tag{20}$$

$$\mu_{[\alpha],t} \sim Normal(0, 1) \tag{21}$$

and

$$\sigma_{[\psi],t} \sim gamma(1,1). \tag{22}$$

Remaining priors were informed by data collected outside the focal region. The prior for grid-cell error (Equation 6) was

$$log(\sigma_{[\varepsilon]}) \sim Normal\left(\overline{log(\widehat{\sigma_{[\varepsilon][A]}})}, SD^2_{[I]}\left(log(\widehat{\sigma_{[\varepsilon][A]}})\right)\right), \tag{23}$$

where $log(\widehat{\sigma_{[\varepsilon][A]}})$ are posterior samples of $log(\sigma_{[\varepsilon]})$ from the annual analysis, $\overline{log(\widehat{\sigma_{[\varepsilon][A]}})}$ is the annual analysis posterior mean estimate, and $SD_{[I]}\left(log(\widehat{\sigma_{[\varepsilon][A]}})\right)$ is an inflated variance of annual analysis posterior samples. Because we estimate $\sigma_{[\varepsilon]}$ as a single parameter for the entire species throughout the IMBCR programmatic footprint, $log(\widehat{\sigma_{[\varepsilon][A]}})$ are informed by data from both within and outside the focal region. We therefore inflated $SD\left(log(\widehat{\sigma_{[\varepsilon][A]}})\right)$ to approximate removal of information from within the focal region using

$$SD_{[I]} = \sqrt{(SD \times n_{all}/n_{discount})}, \tag{24}$$

where SD is the uninflated standard deviation of posterior samples, n_{all} is the program wide sample size (number of grid cells times the number of years), and $n_{discount}$ is the sample size for data collected outside the focal region. Priors for detectability components similarly represented posterior estimates from the annual analysis with SD inflated (i.e., precision discounted following Equation 24) to approximate removal of information from within the focal region. Priors for perceptibility parameters were

$$log(\sigma_{[HN]}) \sim Normal\left(\overline{log(\widehat{\sigma_{[HN][A]}})}, SD^2_{[I]}\left(log(\widehat{\sigma_{[HN][A]}})\right)\right), \tag{25}$$

$$log(h) \sim Normal\left(\overline{log(\widehat{h_{[A]}})}, SD^2_{[I]}\left(log(\widehat{h_{[A]}})\right)\right), \tag{26}$$

and

$$b \sim Normal\left(\overline{\widehat{b_{[A]}}}, SD^2_{[I]}(\widehat{b_{[A]}})\right). \tag{27}$$

Priors for availability hyper-parameters governing variability among BCRs and years were

$$\mu_{[p_{ar}]} \sim Normal\left(\overline{\widehat{\mu_{[p_{ar}][A]}}}, SD^2_{[I]}(\widehat{\mu_{[p_{ar}][A]}})\right) \tag{28}$$

and

$$\sigma_{[p_{ar}]} \sim Normal\left(\overline{\widehat{\sigma_{[p_{ar}][A]}}}, SD^2_{[I]}(\widehat{\sigma_{[p_{ar}][A]}})\right). \tag{29}$$

3.4 Density, abundance, and trend

We derive density estimates for stratum i as

$$D_{it} = \frac{exp(\alpha_{it}) \times \psi_{it} \times \hat{\bar{s}}}{K \times \sum_{d=1}^{d_{[max]}} A_d}, \tag{30}$$

where $K \times \sum_{d=1}^{d_{[max]}} A_d$ is the effective area (km^2) of estimation for a grid cell and $\hat{\bar{s}}$ is the estimated mean size for independent clusters. We sampled $\hat{\bar{s}}$ from the distribution

$$\hat{\bar{s}} \sim TNormal(\hat{\mu_{[s]}}, \widehat{SE_{[s]}}^2, 1, \infty), \tag{31}$$

where $\hat{\mu_{[s]}} = Mean(s)$ and $\widehat{SE_{[s]}} = SD(s)/\sqrt{n}$, in which s represents observed cluster sizes for the species and n is the number of independent clusters detected. We also truncate the sampled distribution so that $\hat{\bar{s}} \geq 1$. We can then estimate population abundance for stratum i as

$$N_{it} = D_{it} \times A_i, \tag{32}$$

where A_i is the area of the stratum. We can then add up the abundances for all strata within a superstratum to estimate abundance for the superstratum (e.g., Colorado, Wyoming, or agency-specific superstrata). For any stratum or superstratum i, we derived trend as the least squares regression slope relating year t with $log(D_{it})$ (or the equivalent $log(N_{it})$),

$$r = \frac{\sum_{t=1}^{T} \left((log(\hat{D}_{it}) - \overline{log(\hat{D}_i)}) \times (t - \bar{t}) \right)}{\sum_{t=1}^{T} \left((t - \bar{t})^2 \right)}. \tag{33}$$

We rescaled r to the annual growth rate with

$$\lambda_{[r]} = e^r, \tag{34}$$

where $\lambda_{[r]} = 1$ implies no trend, and percent annual change in density or abundance with

$$\%\Delta D_{[t]} = (\lambda_{[r]} - 1) \times 100, \tag{35}$$

where $\%\Delta D_{[t]} = 0$ implies no trend.

4 Scenario construction

4.1 Simulated populations

Simulated populations represented available data and our objectives. We describe here how we specified populations to be simulated, and then we later describe how we simulated data given populations specified here (see Section 5). When defining simulated populations, we first defined statewide population densities under trends of interest (Section 4.1.1), we then defined the distribution of statewide populations among

strata (Section 4.1.2), and finally we defined stratum-specific occupancy probabilities (i.e., distribution of the population among grid cells within strata) and spatial heterogeneity within strata expressed as grid-cell error rates (Section 4.1.3). The process of defining populations involved sampling from either a probability distribution (i.e., Equation 40) or from a set of possibilities (see Section 4.1.2 and Section 4.1.3). To ensure simulated data represented uncertainty arising from the the sampling processes involved in defining simulated populations, we simulated 10 replicate populations for each population scenario. We then simulated 10 datasets (Section 5) for each population replicate under each population and sampling scenario (n = 100 datasets per scenario).

We specified simulated populations across two time periods: 1) the *observation period* is the time period for which we had population estimates informed by data and 2) the *future period* is the time period during which we had not yet collected data. Sampling during the observation period matched levels implemented during those years (see Section 4.2). IMBCR sampling in Colorado and Wyoming underwent substantial restratifications in 2011 and 2010, respectively, so for simplicity, observation periods excluded those initial years. Thus, observation periods were 2011-2024 for Colorado and 2010-2024 for Wyoming, and the future period was 2025-2034 for both. Hereafter, we use $t_{[obs]}$ and $t_{[fut]}$ to index a year during the observation and future periods, respectively, $T_{[obs]}$ and $T_{[fut]}$ denotes the max number of years in each period, and $T = T_{[obs]} + T_{[fut]}$. For several parameters, we wanted simulated populations to vary among $t_{[fut]}$ in a manner that resembled variability among $t_{[obs]}$. For these parameters, we specify index $t_{[sim]}$, whereby

$$t_{[sim]} \begin{cases} = t_{[obs]} & t \leq T_{[obs]} \\ \in_R \{1...T_{[obs]}\} & t > T_{[obs]} \end{cases}, \tag{36}$$

and $\in_R$ indicates random sampling with replacement. Thus, parameters indexed by $t_{[sim]}$ would retain their values during the observation period and take on values during the future period that are sampled from observation-period values.

4.1.1 Statewide densities and trends

We defined population scenarios by describing population densities for each year of the simulated monitoring period, which we assumed were a product of a simulated trend and annual variation around that trend. We simulated seven trends: $r \in \{-0.051, -0.03, -0.015, 0, 0.015, 0.03, 0.049\}$ (i.e., $\%\Delta D_{[t]} \in \{-5, -3, -1.5, 0, 1.5, 3, 5\}$). For all population scenarios, we assumed statewide population densities during the observation period equaled statewide posterior median density estimates from the annual analysis for corresponding years,

$$D_{[state],t_{[obs]}} = \widetilde{D_{[state][A],t_{[obs]}}}. \tag{37}$$

To determine future-period densities, we anchored the simulated trend to observation-period densities and defined annual variation around that trend based on the deviations of observation-period densities from the simulated trend line. We started by fitting a trend to $D_{[state],t_{[obs]}}$ using least squares regression (Equation 33 and Equation 35). We then calculated densities predicted along this trend line ($D_{[r][state][observed],t_{[obs]}}$), and we aligned the intercept for the simulated trend by setting

$$D_{[r][state],\overline{t_{[obs]}}} = \overline{\widetilde{D_{[r][state][observed],t_{[obs]}}}}, \tag{38}$$

where $D_{[r][state],\overline{t_{[obs]}}}$ is the predicted statewide population density along the proposed trend line at the center of the observation period symbolized as $\overline{t_{[obs]}}$ (2017.5 for Colorado and 2017 for Wyoming), and $\overline{\widetilde{D_{[r][state][observed],t_{[obs]}}}}$ is the mean of posterior median predicted densities along the observed trend line. Thus, we set the intercept of the proposed trend so that it intersected the observed trend at $\overline{t_{[obs]}}$. We then calculated yearly densities predicted along the proposed trend line as

$$D_{[r][state],t} = \begin{cases} \frac{D_{[r][state],\overline{t_{[obs]}}}}{(\lambda_{[r][state]})^{|t-\overline{t_{[obs]}}|}} & t < \overline{t_{[obs]}} \\ D_{[r][state],\overline{t_{[obs]}}} \times (\lambda_{[r][state]})^{t-\overline{t_{[obs]}}} & t \geq \overline{t_{[obs]}} \end{cases}. \tag{39}$$

We assumed annual deviations of future-period state-level densities from the trend line would resemble annual deviations during the observation period. Thus, we simulated statewide densities for the future period as

$$D_{[state],t_{[fut]}} \sim Normal(D_{[r][state],t_{[fut]}}, SD_{[AnnVar]}), \tag{40}$$

where $SD_{[AnnVar]} = SD(D_{[state],t_{[obs]}} - \widehat{D_{[state],t_{[obs]}}})$.

4.1.2 Distribution of statewide populations among strata

Having determined statewide populations in each year, $D_{[state],t}$, we needed to distribute statewide populations among strata. We initially tried aligning strata-level densities during the observation period to their respective posterior median estimates just as we had done for statewide densities (see Equation 37). However, strata-level and statewide abundances are fundamentally related whereby

$$N_{[state],t} = \sum_{i=1}^{I} N_{it}, \tag{41}$$

where $N_{[state],t}$ and N_{it} are statewide and strata-level abundances, respectively, and $N = D * A$, where A is the area of the stratum or state. Posterior samples $\widehat{N_{[A],it}}$ and $\widehat{N_{[state][A],t}}$ maintain this fundamental relationship, whereas posterior median estimates did not. Thus, we could not use posterior median estimates as true values for strata-level densities for simulated populations. Instead, we calculated the proportion of statewide populations distributed among strata for each posterior sample,

$$p_{[N],itg} = \frac{\widehat{N_{[A],itg}}}{\widehat{N_{[state][A],tg}}}, \tag{42}$$

and for each observation-period year, we identified the posterior sample closest to posterior median estimates for strata-level densities,

$$g_{[select],t_{[sim]}} = g_t \Big| \Big(\sum_{i=1}^{I} (N_{it_{[sim]}g} - \widetilde{N_{it_{[sim]}}}) = \min_{g=1}^{G} \Big(\sum_{i=1}^{I} (N_{it_{[sim]}g} - \widetilde{N_{it_{[sim]}}}) \Big) \Big). \tag{43}$$

Note that because $g_{[select],t_{[sim]}}$ is indexed by $t_{[sim]}$, values in future years for this parameter represent a random selection of observation-year values (see Equation 36). Thus, we used $\mathbf{p}_{[\mathbf{N}],\mathbf{t}_{[\mathbf{sim}]}\mathbf{g}_{[\mathbf{select}],\mathbf{t}_{[\mathbf{sim}]}}}$ to distribute the statewide population among strata, and so stratum-level densities were

$$D_{it_{[sim]}} = \frac{N_{[state],t_{[sim]}} \times p_{[N],it_{[sim]}g_{[select],t_{[sim]}}}}{A_i}, \tag{44}$$

where A_i is the area of stratum i. With this approach, we distributed the population among strata during the future period in a manner that reflected observation-period population distributions while allowing annual variability in the distribution across strata. Note that because we assumed the species only occurred in strata where they were detected at least once over the course of the program, the set of strata across which the population was simulated was invariably a subset of the strata representing the state.

4.1.3 Grid-cell occupancy and error

Two additional parameters defined simulated populations, additional (primarily) spatial variation in density expressed as grid-cell error, $\sigma_{[\varepsilon]}$ in Equation 6, and the grid-cell occupancy rate, ψ_{it} in Equation 2. For simulated populations, we specified a grid-cell error value for each stratum as

$$\sigma_{[\varepsilon],i} = SD(\widetilde{\varepsilon_{[A],i}}), \tag{45}$$

where $SD(\widetilde{\varepsilon_{[A],i}})$ is the standard deviation of posterior median estimates of grid-cell deviations from the stratum mean density. For occupancy, we set

$$\psi_{it_{[sim]}} = \widetilde{\psi_{[A],it_{[sim]}}}, \tag{46}$$

with $t_{[sim]}$ defined in Equation 36.

4.1.4 Realized trends

For evaluation of trend estimator properties (Section 6), we calculated realized trends, $r_{[real]}$, by applying Equation 33 to simulated densities across the observation and future periods ($D_{[state],t}$ and D_{it}). Because we fixed observation period densities to their (posterior median estimated) observed values, $r_{[real]}$ differed somewhat from the simulated trend (hereafter $r_{[sim]}$). We primarily compared simulated trend estimates to $r_{[real]}$ for evaluating estimator properties (i.e., bias and coverage), although we also tracked $r_{[sim]}$ for context.

4.2 Sampling scenarios

Our simulations only described simulated populations at sampled grid cells, so it is necessary to describe sampling scenarios to fully describe simulation methods and structure. Sampling scenarios varied along two

axes, *sampling effort* is the total number of grid cells sampled across all strata and *sampling distribution* is the proportion of effort distributed among strata. Considering our objectives, sampling effort and distribution only varied during the future period and were held constant during the observation period across all sampling scenarios at levels matching historical sampling. Under the baseline scenario for the future period, the number of grid cells in each stratum equaled that stratum's median annual number of grid cells surveyed during the observation period, rounded down; baseline effort is the sum of these stratum-level values, and baseline distribution is each stratum's share of that total. We provide further details and rationale for sampling scenarios in the main body of this report.

5 Data simulation

We simulated 100 datasets per (population and sampling) scenario (10 datasets per simulated population) using the analysis model described in Section 3 with population parameter values established in Section 4.1. We simulated the number of independent clusters (see Section 3.1 for definition of a cluster) present within the sampled area of a grid cell as

$$N_{[c][sim],ijt} \sim Poisson(\lambda_{[N][sim],ijt} \times z_{[sim],ijt} \times A_{[s]}). \tag{47}$$

The three components of the Poisson rate for $N_{[c][sim],ijt}$ are the expected Poisson rate (clusters per km^2) at occupied grid cells ($\lambda_{[N][sim],ijt}$), a binary indicator of whether the grid cell is occupied ($z_{[sim],ijt}$), and the area (km^2) effectively sampled within the grid cell $A_{[s]}$. We calculated the expected conditional Poisson rate as

$$\lambda_{[N][sim],ijt} = exp\left(log\left(\frac{D_{it_{[sim]}}}{\overline{s_{[A]}} \times \psi_{it}}\right) + \epsilon_{jt}\right), \tag{48}$$

where $D_{it_{[sim]}}$ and ψ_{it} arise from Equation 44 and Equation 46, respectively, $\overline{s_{[A]}}$ is the mean of all recorded cluster sizes within the state, and ϵ_{jt} is the grid-cell deviation from the stratum-specific mean simulated from a normal distribution with standard deviation from Equation 45, $\epsilon_{jt} \sim Normal(0, \sigma^2_{[\varepsilon],i})$. We simulated the occupancy state of a grid cell as

$$z_{[sim],ijt} \sim Binomial(\psi_{it}), \tag{49}$$

and the sampled area within the grid cell was

$$A_{[s]} = K \times \sum_{d=1}^{d_{[max]}} A_d, \tag{50}$$

where $\sum_{d=1}^{d_{[max]}} A_d$ is the sum of the areas of all distance bins for the species.

Having simulated abundance at the grid cell, we simulated counts of independent clusters and the distribution of counted clusters among distance and time-removal bins. We simulated the total number of clusters counted at a sampled grid cell as

$$n_{[sim],ijt} \sim Binomial\left(N_{[c][sim],ijt}, p_{[a][sim],lt} \times p_{[p][sim]} \times \frac{K_{[s][sim],ijt}}{K}\right), \tag{51}$$

where $p_{[sim][a],lt}$, $p_{[p][sim]}$, and $K_{[s][sim],ijt}$ are analogous to availability ($p_{[a],lt}$), perceptibility ($p_{[p]}$), and sampling effort ($K_{[s],ijt}$) terms in Equation 7. Parameter values for detectability components were set to posterior median estimates from the annual analysis:

$$p_{[a][sim],lt} = \widetilde{p_{[a][A],lt_{[sim]}}} \tag{52}$$

and

$$p_{[p][sim]} = \widetilde{p_{[p][A]}}. \tag{53}$$

For sampling effort,

$$K_{[s][sim],ijt} \begin{cases} = K_{[s],ijt} & t \leq T_{[obs]} \\ \in_R \mathbf{K}_{[s]} & t > T_{[obs]} \end{cases}, \tag{54}$$

where $\mathbf{K}_{[s]}$ is the set of all values for $K_{[s],ijt}$ during the observation period and $\in_R$ indicates random sampling with replacement. We simulated the distribution of counted clusters among distance and time-removal bins as

$$\mathbf{y}_{[a][sim],ijt} \sim Multinomial\left(n_{[sim],ijt}, \boldsymbol{\pi}^{[c]}_{[a][sim],tl}\right) \tag{55}$$

and

$$\mathbf{y}_{[p][sim],ijt} \sim Multinomial\left(n_{[sim],ijt}, \boldsymbol{\pi}^{[c]}_{[p][sim],tl}\right), \tag{56}$$

where $\boldsymbol{\pi}^{[c]}_{[a][sim],tl}$ and $\boldsymbol{\pi}^{[c]}_{[p][sim],tl}$ are analogous to $\boldsymbol{\pi}^{[c]}_{[a],tl}$ and $\boldsymbol{\pi}^{[c]}_{[p],tl}$ in Equation 10 and Equation 11, respectively, calculated from from $p_{[p][sim]}$ and $p_{[p][sim]}$ using Equation 12, Equation 14, Equation 15, and Equation 16.

6 Data analysis

We analyzed simulated data using the model described above (Section 3), and then generated simulated estimates of density and trend. We estimated power to discern a trend ($[1-\beta]_{[r]}$) as the proportion of simulations when the 80%, 90%, or 95% credible interval for $\hat{r}$ excluded a flat trend ($r = 0$). We estimated two forms of power,

$$[1-\beta]_{[r][+]} = \frac{\sum_{x=1}^{100} \begin{cases} CI_{[lower]}(\hat{r}) > 0 & r_{[real]} > 0 \\ CI_{[upper]}(\hat{r}) < 0 & r_{[real]} < 0 \end{cases}}{100} \tag{57}$$

is the probability of discerning a trend in the direction of the true trend, which we can refer to as *true power*, and

$$[1-\beta]_{[r][-]} = \frac{\sum_{x=1}^{100} \begin{cases} CI_{[lower]}(\hat{r}) > 0 & r_{[real]} \leq 0 \\ CI_{[upper]}(\hat{r}) < 0 & r_{[real]} \geq 0 \end{cases}}{100} \tag{58}$$

is the probability of discerning a trend in the direction opposite the true trend, referred to hereafter as *false power*. For the trend estimator to be informative, we want high true power and low false power. We also estimated bias and coverage for both trend and density estimators. We calculated bias as

$$Bias(\hat{r}) = \overline{\hat{r_x} - r_{[real]}} \tag{59}$$

and

$$Bias(\hat{D}) = \overline{\hat{D}_x - D}. \tag{60}$$

We calculated coverage of the trend estimator as

$$Coverage(\hat{r}) = \frac{\sum_{x=1}^{100} \left(CI_{[low]}(\hat{r_x}) < r_{[real]} \text{ and } CI_{[high]}(\hat{r_x}) > r_{[real]} \right)}{100}. \tag{61}$$

We did unfortunately find substantial bias in density ($Bias(\hat{D})$) and trend estimates ($Bias(\hat{r})$) under a substantive number of scenarios, and we were unable to determine the source of this bias, nor were we able to find any descriptions of bias in the literature that could explain observed bias. We did not find any substantive correlation or relationship between $Bias(\hat{r})$ and $Bias(\hat{D})$, although $Bias(\hat{D})$ was negatively related with D, which is not a pattern that we found documented or explained in published literature. Not having identified the source of these biases, we remain uncertain whether these biases accurately represent estimator properties or if they are an artifact of our simulation approach. We therefore generated bias-corrected power estimates, whereby we implemented the analysis of simulated estimates above, retrieved scenario-specific estimates of bias from the initial analysis, and then subtracted estimated bias from initial estimates to generate bias-corrected estimates of trend. We then calculated statistical power for bias-corrected trend estimates and drew stronger inference of power relationships with sampling effort and distribution where estimated relationships were consistent regardless of bias correction.

References

Timmer, Jennifer M., Jessie A. Reese, Matthew F. McLaren, et al. 2026. *Integrated Monitoring in Bird Conservation Regions (IMBCR): 2025 Field Season Report*. Bird Conservancy of the Rockies. https://bird-conservancy-of-the-rockies.github.io/IMBCR_AnnualReport_2025/.